General Amino Acid Control and 14-3-3 Proteins Bmh1/2 Are Required for Nitrogen Catabolite Repression-Sensitive Regulation of Gln3 and Gat1 Localization

Jennifer J. Tate, David Buford, Rajendra Rai, and Terrance G. Cooper[1]
Department of Microbiology, Immunology, and Biochemistry, University of Tennessee Health Science Center, Memphis, Tennessee 38163

ABSTRACT Nitrogen catabolite repression (NCR), the ability of *Saccharomyces cerevisiae* to use good nitrogen sources in preference to poor ones, derives from nitrogen-responsive regulation of the GATA family transcription activators Gln3 and Gat1. In nitrogen-replete conditions, the GATA factors are cytoplasmic and NCR-sensitive transcription minimal. When only poor nitrogen sources are available, Gln3 is nuclear, dramatically increasing GATA factor-mediated transcription. This regulation was originally attributed to mechanistic Tor protein kinase complex 1 (mTorC1)-mediated control of Gln3. However, we recently showed that two regulatory systems act cumulatively to maintain cytoplasmic Gln3 sequestration, only one of which is mTorC1. Present experiments demonstrate that the other previously elusive component is uncharged transfer RNA-activated, Gcn2 protein kinase-mediated general amino acid control (GAAC). Gcn2 and Gcn4 are required for NCR-sensitive nuclear Gln3-Myc^{13} localization, and from epistasis experiments Gcn2 appears to function upstream of Ure2. Bmh1/2 are also required for nuclear Gln3-Myc^{13} localization and appear to function downstream of Ure2. Overall, Gln3 phosphorylation levels decrease upon loss of Gcn2, Gcn4, or Bmh1/2. Our results add a new dimension to nitrogen-responsive GATA-factor regulation and demonstrate the cumulative participation of the mTorC1 and GAAC pathways, which respond oppositely to nitrogen availability, in the nitrogen-responsive control of catabolic gene expression in yeast.

KEYWORDS Bmh1/2; Gat1; Gcn2; Gln3; nitrogen catabolite repression

WHEN simultaneously provided with both a good and poor nitrogen source, *Saccharomyces cerevisiae* cells will exhaust the good source from the medium before using the poor one (Watson 1977). However, there is no particular structural requirement for a compound to function as a good nitrogen source beyond being present in sufficient amounts, and transported and catabolized rapidly. These requirements result in the quality of a nitrogen source being somewhat dependent on the strain background analyzed. The regulatory system mediating this selectivity is designated nitrogen catabolite repression (NCR) (Cooper 1982, 2004; Broach 2012; Ljungdahl and Daignan-Fornier 2012; Conrad *et al.* 2014). The functional heart of NCR is the GATA factors, Gln3 and Gat1, which activate the transcription of genes needed to transport and catabolize poorly used nitrogen sources. In nitrogen-replete conditions, Gln3- and Gat1-mediated transcription is repressed, whereas it is derepressed when nitrogen supplies are meager.

Mechanism of TorC1-mediated Gln3 regulation

Once GATA factors were identified and the transcriptional wiring of NCR-sensitive transcriptional control elucidated (Hofman-Bang 1999; Cooper 2002, 2004; Magasanik and Kaiser 2002), the pressing question became how the response to such a breadth of compounds could be integrated and directed to regulate Gln3 and Gat1. The answer began to emerge by connecting the dots between Gln3 and its negative regulator, Ure2, with mechanistic Tor protein kinase complex 1 (mTorC1) (Blinder *et al.* 1996; Beck and Hall 1999; Cardenas *et al.* 1999; Hardwick *et al.* 1999; Bertram *et al.* 2000; Kulkarni *et al.* 2001; Carvalho and Zheng 2003). This

doi: 10.1534/genetics.116.195800
Manuscript received September 11, 2016; accepted for publication December 21, 2016; published Early Online December 22, 2016.
[1]Corresponding author: Department of Microbiology, Immunology and Biochemistry, University of Tennessee Health Science Center, 858 Madison Ave., Memphis, TN 38163. E-mail: tcooper@uthsc.edu

global regulator integrates and generates responses to a diverse spectrum of nutrient- and stress-related inputs (Crespo and Hall 2002; Kim and Guan 2011; Loewith and Hall 2011; Laplante and Sabatini 2012; Lamming and Sabatini 2013; Bar-Peled and Sabatini 2014; Swinnen *et al.* 2014; Shimobayashi and Hall 2016; Stauffer and Powers 2016). When activated, mTorC1 upregulates processes associated with increased cell division, *e.g.*, protein or ribosomal protein synthesis; and conversely downregulates those associated with nutrient limitation, *e.g.*, NCR-sensitive transcription and autophagy. In nutrient-poor conditions the regulatory outcomes are reversed.

Models conceptualizing this and observations from subsequent investigations posit that excess nitrogen or glutamine activates mTorC1 via the intermediate action of a leucyl transfer RNA (tRNA)-Ego-Gtr complex (figure 1 in Rai *et al.* 2016) (Binda *et al.* 2009, 2010; Bonfils *et al.* 2012; Crespo *et al.* 2002). Thus activated, mTorC1 phosphorylates Gln3 and Tor-associated protein, Tap42 (Di Como and Arndt 1996; Beck and Hall 1999; Bertram *et al.* 2000). Phosphorylation of Gln3 facilitates its interaction with Ure2, sequestering it in the cytoplasm (Bertram *et al.* 2000). Tap42 phosphorylation facilitates its interaction with the Sit4 and PP2A phosphatases (Di Como and Arndt 1996; Jiang and Broach 1999). The Tap42-phosphatase complexes, bound to mTorC1, result in their inactivation; further maintaining Gln3 in its phosphorylated, Ure2-bound form (Beck and Hall 1999; Bertram *et al.* 2000; Wang *et al.* 2003; Yan *et al.* 2006). In limiting nitrogen or after rapamycin inhibition of mTorC1, the Tap42-Sit4 complex is released and thus activated, and it dephosphorylates Gln3; permitting it to dissociate from Ure2, enter the nucleus, and activate NCR-sensitive transcription (Beck and Hall 1999; Bertram *et al.* 2000; Wang *et al.* 2003; Yan *et al.* 2006) .

Need to enlarge the mTorC1 control model

As elegant and engaging as this model is, it has become increasingly clear that nitrogen-responsive mTorC1 regulation was insufficient to explain NCR (Cox *et al.* 2004a,b; Tate *et al.* 2006, 2009, 2010; Georis *et al.* 2008, 2011a,b; Fayyad-Kazan *et al.* 2016). Most significantly, the five methods interchangeably used to downregulate mTorC1 activity in fact represented five physiologically distinct conditions when a single reporter, Gln3, was employed (Tate and Cooper 2013): Rap-elicited nuclear Gln3 localization required both Sit4 and PP2A phosphatases. A similar Gln3 response to growth in derepressive proline medium or following short-term nitrogen starvation required only Sit4. On the other hand, long-term nitrogen starvation (correlating with G1 arrest) or nuclear Gln3 localization in response to the glutamine synthetase inhibitor, methionine sulfoximine (Msx), required neither phosphatase. Most telling, Gln3 intracellular localization was immune to leucine starvation, leucyl tRNA synthetase inhibitors, or abolishment of the Gtr-Ego complex components needed to activate mTorC1 (Tate and Cooper 2013; Tate *et al.* 2015a).

Parsing Gln3 regulation with Gln3 substitution mutants

Recent experiments have begun to parse and identify the missing regulatory components and mechanisms that cumulatively achieve NCR-sensitive Gln3 control. The construction of Gln3 substitutions uniquely abolishing the Gln3 response to one of the above five conditions while leaving others untouched has been pivotal to this progress. Alteration of $Gln3_{656–662}$ (pRR850) abolishes its interaction with mTor1 and response to rapamycin. This results in cytoplasmic Gln3 sequestration in a nitrogen-replete medium decreasing by half, with Gln3 about equally distributed as cytoplasmic, nuclear-cytoplasmic, and nuclear (Rai *et al.* 2013). Alterations in $Gln3_{526–539}$ (pRR1045) eliminates a response to rapamycin without any other effects (Rai *et al.* 2014) and alanine substitutions in $Gln3_{477–497}$ (pRR680) diminishes cytoplasmic Gln3 sequestration by half in nitrogen-rich yeast nitrogen base (YNB)-glutamine medium, accompanied by the characteristic tripartite distribution, but without further effects (Rai *et al.* 2016). When the alanine substitutions in $Gln3_{477–497}$ (pRR680) were combined by those in the Gln3-mTor1 interaction site (pRR850), they additively eliminated cytoplasmic Gln3 sequestration in cells provided with excess nitrogen. In other words, the distinct regulatory systems acting through these two Gln3 target sites cumulatively controlled Gln3 localization (Rai *et al.* 2016). It was paradoxical, however, that the Gln3 response to glutamine starvation (Msx treatment) was not affected by any of the above *gln3*-substitution mutants because mTorC1 activity had been reported to be regulated by glutamine (Crespo *et al.* 2002). How was glutamine regulating Gln3 localization?

The question was answered by investigating the phenotypes of several *gln3* "nuclear export" mutants. The data obtained demonstrated that once Gln3 enters the nucleus, its intranuclear path is regulated by glutamine levels themselves or by those of a glutamine metabolite able to be mimicked by glutamine analogs (Rai *et al.* 2015). In high glutamine, Gln3 can exit from the nucleus in the absence of binding to its promoter GATA targets. In contrast, when glutamine levels are decreased, nuclear Gln3 export can no longer occur in the absence of functional DNA binding.

Candidates to join mTorC1 in cumulative Gln3 regulation

The clear demonstration that overall cumulative Gln3 regulation could be parsed with *gln3* mutations provided the requisite information needed to search for proteins, other than mTorC1, required to achieve Gln3 control. What nitrogen-responsive regulators might be candidates, especially molecules not previously associated with overall NCR-sensitive transcription or Gln3 localization? Among the potential candidates were the general amino acid control (GAAC) pathway and the 14-3-3 phospho-protein binding proteins Bmh1/2 (Cherkasova and Hinnebusch 2003; van Heusden and Steensma 2006; van Heusden 2009).

Nitrogen-responsive GAAC and 14-3-3 proteins

Amino acid starvation increases the cellular levels of uncharged tRNAs (Staschke *et al.* 2010). These uncharged tRNAs can then bind to a histidyl tRNA synthetase-related domain of the protein kinase, Gcn2, and activate it (Cherkasova and Hinnebusch 2003; Hinnebusch 2005; Castilho *et al.* 2014; Lageix *et al.* 2015; Dever *et al.* 2016). Activated Gcn2 phosphorylates Ser51 of eIF2αP. Phosphorylated eIF2α-P inhibits the guanine exchange factor eIF2B required for conversion of eIF2-GDP to eIF2-GTP, which in turn is required for protein synthesis initiation. Hence decreased tRNA levels and correspondingly increased Gcn2 activity decreases the rate of protein synthesis. Activated Gcn2 also stimulates Gcn4 translation. Gcn4 is the transcription factor responsible for stimulating expression of >500 genes, including those of amino acid biosynthesis (Garcia-Barrio *et al.* 2000; Krishnamurthy *et al.* 2001; Hinnebusch 2005; Natarajan *et al.* 2001 Staschke *et al.* 2010). Gcn4 additionally participates in combination with Gln3 to coactivate transcription of a small number of specific NCR-sensitive genes whose promoters contain Gcn4 binding sites (Mitchell and Magasanik 1984; Natarajan *et al.* 2001; Valenzuela *et al.* 2001, data set URL is no longer active; Riego *et al.* 2002; Sosa *et al.* 2003; Staschke *et al.* 2010; Hernández *et al.* 2011). On the other hand, when charged tRNAs are in excess, Gcn2-mediated regulatory outcomes are reversed. Importantly, nitrogen conditions that activate mTorC1 are opposite to those required to activate Gcn2.

The Bmh1/2 proteins are involved in a wide variety of control pathways by virtue of binding to and positively or negatively regulating phosphorylated regulatory molecules ranging from Adr1, at the level of transcription (Parua *et al.* 2010; Parua and Young 2014), to their participation in Mks1-dependent negative regulation of nuclear Rtg1/3 localization and retrograde transcription (Liu *et al.* 2003, 2005).

Materials and Methods

Strains and culture conditions

The *S. cerevisiae* strains used in this work appear in Table 1. Experiments measuring the effects of abolishing Gcn2 were performed in the BY4742 background. Those associated with loss of Bmh1/2 employed Σ1278b derivative because this is one of the very few strain backgrounds where a *bmh1*Δ,*bmh2*Δ double mutant is able to grow (Roberts *et al.* 1997; Robertson *et al.* 2000). Transformants, prepared by the lithium acetate method (Ito *et al.* 1983), were used as soon as possible after transformation (5 days or less). Yeast strains for the *gcn2*Δ, *ure2*Δ epistasis experiment were generated using the primers in Table 2 using the method of Wach *et al.* (1994).

Cultures (50 ml) were grown to midlog phase ($A_{600\ nm}$ = 0.3–0.5) in YNB (without amino acids or ammonia; Difco, Detroit, MI) minimal medium containing the indicated nitrogen source (final concentration 0.1%). *gcn2*Δ*ure2*Δ mutant cells were harvested at $A_{600\ nm}$ = ~0.4. Leucine (120 μg/ml), histidine (20 μg/ml), lysine (40 μg/ml), tryptophan (20 μg/ml), and uracil (20 μg/ml) were added as needed to cover auxotrophic requirements. Cells were treated with 200 ng/ml of rapamycin for 15 min (Gcn2 experiments) or 20 min (Bmh1/2 experiments) and for 30 min with 2 mM Msx as described Georis *et al.* (2011).

Table 1 Strains used in this work

Strain	Pertinent genotype	Complete genotype
10560-2B	Wild type	*MATa*, *ura3-52*, *his3*::*hisG*, *leu2*::*hisG*
RRY1216	*bmh1*Δ,*bmh2*Δ	*MATa*, *ura3-52*, *bmh1*Δ::*His3*, *bmh2*Δ::*His3*, *his3*, *leu2*
BS0033a	*ure2*Δ,*bmh1*Δ, *bmh2*Δ	*Mata*, *ura3*, *leu2*, *trp1*, *his3 bmh1*Δ::*His3*, *bmh2*Δ::*His3*
RR114	*ure2*Δ	*MATα*, *lys2*, *ura3*, *trp1*, *ure2*::*TRP1*
BY4742	Wild type	*MATα*, *his3*Δ, *leu2*Δ, *lys2*Δ, *ura3*Δ
GCN2[a]	*gcn2*Δ	*MATα*, *his3*Δ, *leu2*Δ, *lys2*Δ, *ura3*Δ, *gcn2*Δ::*KanMX*
GCN4[a]	*gcn4*Δ	*MATα*, *his3*Δ, *leu2*Δ, *lys2*Δ, *ura3*Δ, *gcn4*Δ::*KanMX*
RR259	*ure2*Δ	*MATα*, *his3*Δ, *leu2*Δ, *lys2*Δ, *ura3*Δ, *ure2*Δ::*NatMX*
JT11	*gcn2*Δ,*ure2*Δ	*MATα*, *his3*Δ, *leu2*Δ, *lys2*Δ, *ura3*Δ, *gcn2*Δ::*KanMX*, *ure2*Δ::*NatMX*

[a] Obtained from transOMIC Technologies. Deletion was independently validated as described in *Materials and Methods*.

Plasmid construction

Gln3-Myc[13] plasmids pRR536, pRR680, pRR850, pRR1045, and pRR1194, and Gat1-Myc[13] plasmid pKA62 were constructed in *CEN*-based vectors and have been previously described (Liu *et al.* 2003; Kulkarni *et al.* 2006; Rai *et al.* 2013, 2014, 2016). All plasmids contained a full-length *GLN3* or *GAT1* gene whose transcription was driven by its native wild-type promoter. The structures of all constructs were verified by restriction mapping and DNA sequence analyses.

Gln3-Myc[13], Gat1-Myc[13], and Gln3-GFP localization

Cell collection and Gln3-Myc[13] and Gat1-Myc[13] visualization by indirect immunofluorescent microscopy were performed as described (Cox *et al.* 2002, 2004a,b; Tate *et al.* 2006, 2009; Georis *et al.* 2008; Tate and Cooper 2013). All cell images were collected as described earlier (Tate *et al.* 2010; Rai *et al.* 2013, 2014). pRS416-Gln3-GFP (Liu *et al.* 2003) was monitored in growing *bmh1*Δ,*bmh2*Δ mutant cultures as described in the text.

Image processing

Microscopic images for presentation were prepared using Adobe Photoshop and Illustrator programs. Level settings (shadow and highlight only) were altered where necessary to avoid any change or loss in cellular detail relative to that observed in the microscope; changes were applied uniformly to the image presented and were similar from one image to another. Midtone gamma settings were never altered. These processed images were used for illustrative presentation only, *not* for scoring Gln3-Myc[13], Gat1-Myc[13], or Gln3-GFP intracellular distributions.

Table 2 Oligonucleotides used in this work

Use	Oligonucleotide sets
*gcn2*Δ,*ure2*Δ construction	*ure2-natMX*-forward 5′-GTCATATTGTTTTAAGCTGCAAATTAAGTTGTAC ACCAAATGCGTACGCTGCAGGTCGAC-3′ *ure2-natMX*-reverse 5′-CCTCCTTCTTCTTTCTTTCTTGTTTTTAAACAGCC TTCAATCGATGAATTCGAGCTCG-3′
*gcn2*Δ,*ure2*Δ verification	*ure2* forward ATG 5′-GCTTCCTTACTCGAGGTTG-3′ *ure2* reverse Nat 5′-GGATGTGATGTGAGAACTG-3′ *ure2* forward Nat 5′-CGCTCTACATGAGCATGC-3′ *ure2* reverse TGA 5′-GGAATTCTGTGGTTGGGGTAAC-3′ *ure2* coding forward 5′-CCAAGTGTCGAATCTCTCCA-3′ *ure2* coding reverse 5′-ATCATCGGACCAGAGTAATGG-3′

Determination of intracellular Gln3-Myc[13] and Gat1-Myc[13] distributions

Gln3-Myc^{13} and Gat1-Myc^{13} intracellular localizations were manually scored in 200 or more cells for each data point. Unaltered, primary .zvi image files viewed with Carl Zeiss (Thornwood, NY) AxioVision 3.0 and 4.8.1 software were exclusively used for scoring purposes. Cells containing the tagged proteins were classified into one of three categories, based on where the protein was: cytoplasmic (cytoplasmic fluorescent material only; red histogram bars), nuclear-cytoplasmic (fluorescent material appearing in both the cytoplasm and colocalizing with DAPI-positive material, DNA; yellow bars), or nuclear (fluorescent material colocalizing only with DAPI-positive material; green bars). Representative "standard" images and detailed descriptions of these categories appear in figure 2 of Tate *et al.* (2009) along with descriptions of how the criteria were applied. The precision of our scoring has been repeatedly documented with a SD <10% for $N = 7$–10 experiments performed over 9 months in some cases and up to 3 years in others (Tate *et al.* 2006, 2010; Rai *et al.* 2013, 2014). Experiment-to-experiment variation can also be assessed by comparing data obtained with wild-type pRR536 in transformants cultured in glutamine, glutamine plus rapamycin, proline, ammonia, and ammonia plus Msx since a separate wild-type culture accompanied each of the mutants.

Only two categories (nuclear and nuclear-cytoplasmic) were used to score Gln3-GFP localization because high background fluorescence made it difficult to confidently conclude whether Gln3-GFP localization was nuclear-cytoplasmic *vs.* nuclear.

Images accompanying the histograms were chosen on the basis that they exhibited intracellular tagged protein distributions as close as possible to those observed by quantitative scoring. However, identifying a field that precisely reflected the more quantitative scoring data were sometimes difficult unless the tagged protein was situated in a single cellular compartment.

Northern blot analyses

Yeast strains used for Northern analyses were grown to midlog phase in the indicated medium. Total RNA was isolated as described earlier (Carlson and Botstein 1982; Schmitt *et al.* 1990), and Northern blot analyses performed as described by Cox *et al.* (2004a,b).

Western blot analyses

Extracts for Western blots were prepared and Western analyses were performed as previously described (Cox *et al.* 2004a; Rai *et al.* 2015).

Quantitative RT-PCR analyses

Quantitative RT-PCR (qRT-PCR) analyses were performed as described in Rai *et al.* (2015). *GDH2* and *TBP1* primer sequences were as previously described Georis *et al.* (2008, 2011).

Data availability

See Table 1 for strains and Table 2 for primers used.

Results

Why GAAC might be a good candidate

We previously demonstrated nuclear Gln3-Myc^{13} localization is abolished by alteration of the rare glutamine $tRNA_{CUG}$ (*sup70-65* mutation) at the semipermissive temperature of 30° (Tate *et al.* 2015b). Investigating the more global effects of the mutant, Kemp *et al.* (2013) reported that *sup70-65* $tRNA_{CUG}$ was unstable and inefficiently charged at 30°. These observations suggested the following: (i) one or more events associated with $tRNA_{CUG}$ were required for nuclear Gln3 localization, and (ii) these events were adversely affected in some specific (particular protein or $tRNA_{CUG}$-protein complex) or general (protein synthesis *per se*) way when $tRNA_{CUG}$ was altered. The related finding that cycloheximide inhibition of protein synthesis causes Gln3 to relocate to the cytoplasm (Tate and Cooper 2013) argued in favor of the *sup70-65* effects on overall protein synthesis being potentially pertinent. This focused our attention on work predominantly from the Hinnebusch laboratory which showed that Gcn2 protein kinase is exquisitely sensitive to the levels of charged tRNAs (Garcia-Barrio *et al.* 2000; Cherkasova and Hinnebusch 2003; Hinnebusch 2005), hence making it a possible candidate to explain how the glutamine $tRNA_{CUG}$ *sup70-65* mutation, cycloheximide inhibition of protein synthesis initiation, and repressive nitrogen sources might all function in a common mechanism to regulate nuclear Gln3 localization. This reasoning predicted that inactivating Gcn2 or deleting the nonessential *GCN2* gene would adversely affect nuclear Gln3 localization.

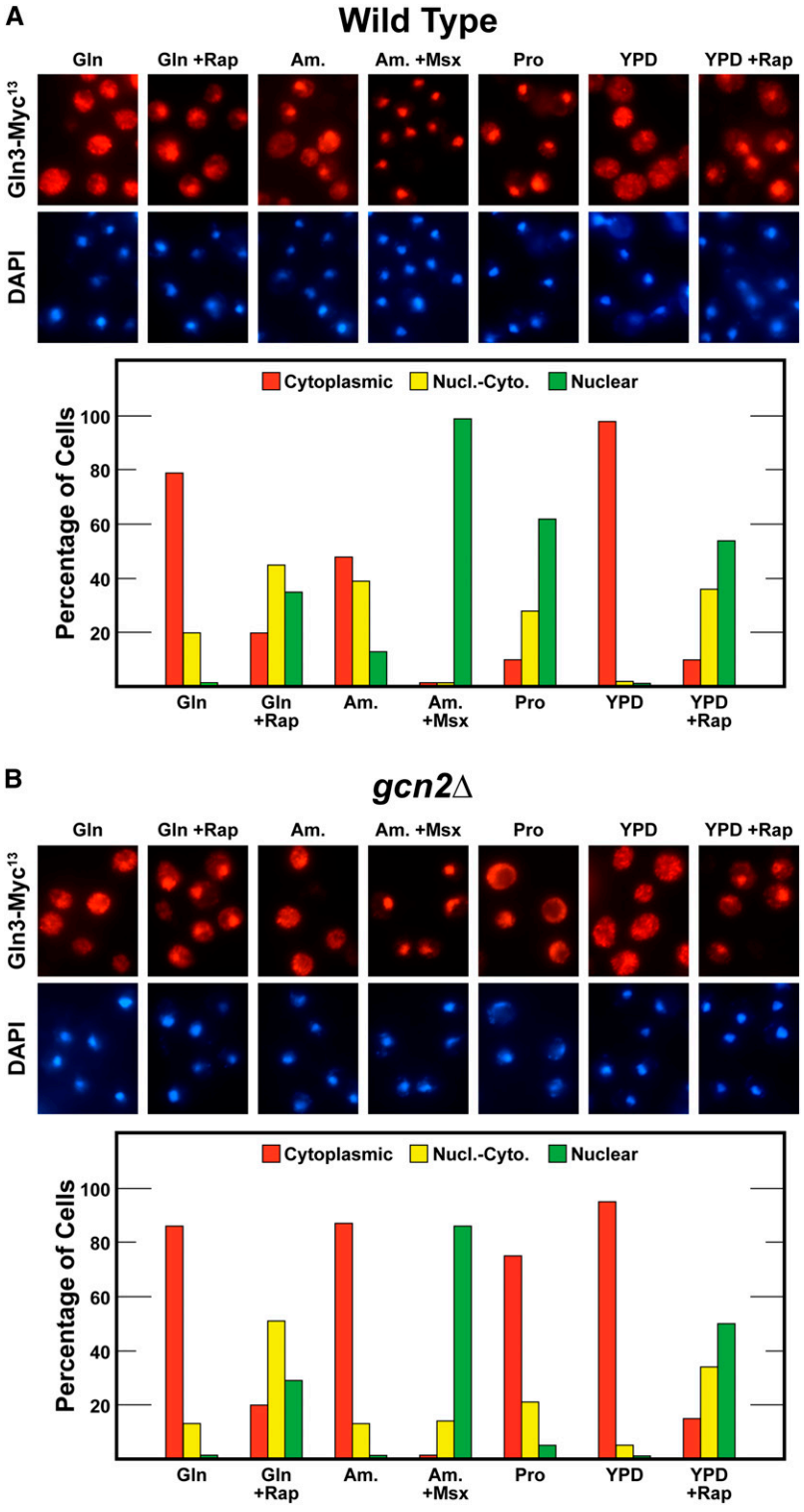

Figure 1 Gcn2 is required for nuclear Gln3-Myc[13] localization in response to growth with nitrogen sources whose use requires NCR-sensitive transcription. Gln3-Myc[13] localization was measured in (A) wild-type (BY4742) and (B) *gcn2*Δ cells cultured in complex YPD or YNB-minimal medium with glutamine (Gln), ammonia (Am.), or proline (Pro) as sole nitrogen source. Rapamycin (+Rap) or methionine sulfoximine (+Msx) were added where indicated to glutamine- or ammonia-grown cells, respectively. Intracellular Gln3-Myc[13] was visualized and scored as cytoplasmic (red bars), nuclear-cytoplasmic (yellow bars), or nuclear (green bars) as described in *Materials and Methods*. Nucl.-Cyto., nuclear-cytoplasmic.

Gcn2 is required for nuclear Gln3-Myc[13] localization during growth with NCR-sensitive nitrogen sources

To test this hypothesis, we compared Gln3-Myc[13] localization in wild type *vs.* *gcn2*Δ cells in response to our standard assay conditions. In repressive YNB-glutamine medium, the Gln3-Myc[13] responses in wild-type and *gcn2*Δ cells were indistinguishable. In contrast, nuclear Gln3-Myc[13] localization was almost completely abolished in ammonia- or proline-grown *gcn2*Δ cells (Figure 1). Consistent with these results, the growth rates of wild-type and *gcn2*Δ cells were relatively similar in repressive YNB-asparagine medium. In contrast, *gcn2*Δ growth was drastically slowed in YNB-proline medium. In other words, the *gcn2*Δ growth characteristics were very similar to those of *gln3*Δ as well as those

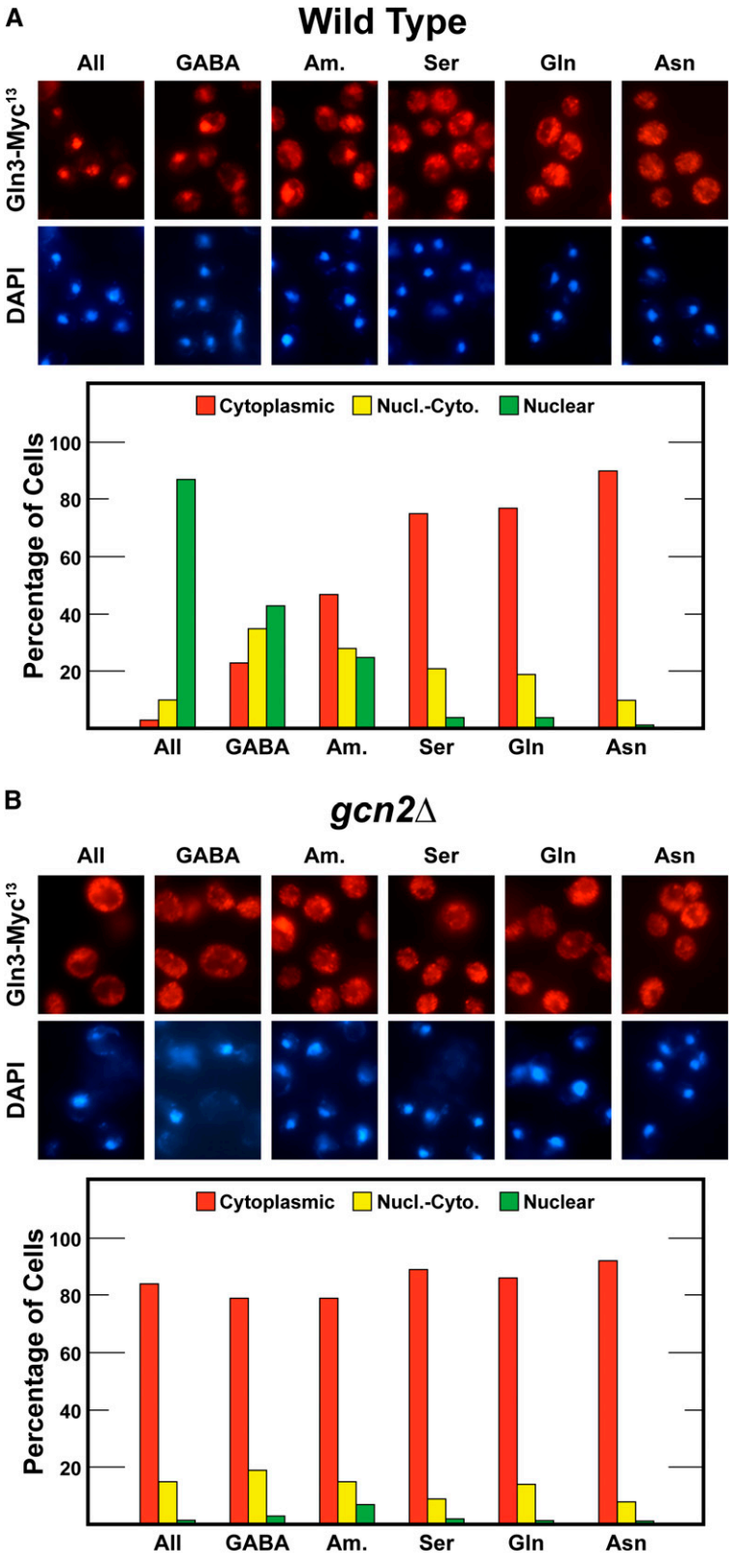

Figure 2 Gcn2 requirement for nuclear Gln3-Myc[13] localization in cells provided with poor, derepressive nitrogen sources. Gln3-Myc[13] localization was measured in (A) wild-type (BY4742) and (B) *gcn2*Δ cells. Nitrogen sources ranged from derepressive to repressive: allantoin (All), γ-amino-butyrate (GABA), ammonia (Am.), serine (Ser), glutamine (Gln), or asparagine (Asn) were provided (final concentration of 0.1%) as sole nitrogen source in YNB-minimal media. The experimental format and data presentation were as in Figure 1. Nucl.-Cyto., nuclear-cytoplasmic.

expected if Gln3 was unable to enter the nucleus in proline-grown cells.

Importantly, the *gcn2*Δ phenotype exhibited high specificity. Gln3-Myc[13] responses to rapamycin or Msx treatment, which have been shown to occur via mTorC1 and glutamine-mediated intranuclear regulation, respectively, were unaffected; they remained the same as wild type (Beck and Hall 1999; Cardenas *et al.* 1999; Hardwick *et al.* 1999; Bertram

et al. 2000; Rai *et al.* 2015). The responses to abolishing Gcn2 were restricted to nitrogen sources whose uptake and/or metabolism depended on NCR-sensitive gene expression. To test this conclusion further, we assayed the effects of *gcn2*Δ on multiple nitrogen sources ranging from derepressive (allantoin, proline) to those that are highly repressive (asparagine, glutamine, serine). The more repressive the nitrogen source, the smaller the effect of deleting *GCN2* on nuclear Gln3 localization (Figure 2). Again the phenotype correlated with that expected of abolishing Gln3 function.

Gcn2 is required for NCR-sensitive transcription

The above results with Gln3-Myc^{13} localization predicted that loss of Gcn2 should also have demonstrable effects on NCR-sensitive transcription. To test this prediction, we measured the steady-state levels of *GDH2* messenger RNA in wild-type and *gcn2*Δ cells cultured in glutamine-, proline-, and allantoin-YNB media as well as in the presence of rapamycin using qRT-PCR (Figure 3). All of the data were compared to wild-type untreated glutamine levels. Abolishing Gcn2 had no demonstrable effect on *GDH2* expression in untreated or rapamycin-treated, glutamine-grown cultures. The expression profile was the same as wild type. In derepressive proline medium, *GDH2* expression increased 40-fold in wild-type cells, but <5-fold in *gcn2*Δ. The *GDH2* transcription results correlated perfectly with the Gln3-Myc^{13} localization data (Figure 3).

In allantoin-grown wild-type cells, *GDH2* expression increased >10-fold relative to the repressed levels and decreased to <5-fold in *gcn2*Δ. The more modest effect of *gcn2*Δ observed in allantoin-grown cells was not unexpected because the main function of *GDH2*-encoded, NAD-dependent glutamate dehydrogenase is the production of ammonia. NCR-sensitive *GDH2* expression is driven by a complex promoter and is known to be greater in medium containing the Gdh2 substrate, glutamate (a product of proline degradation), than it is in ammonia (a product of allantoin degradation) medium (Figure 3) (Miller and Magasanik 1991). Together the data indicated that high-level, NCR-sensitive transcription required Gcn2.

Effects of Gcn2 loss on short- and long-term nitrogen starvation

Another natural condition that triggers nuclear Gln3 localization is nitrogen starvation. The length of starvation, however, is an important parameter. Nuclear Gln3 localization in response to short-term nitrogen starvation (from minutes to 3 or 4 hr depending on the strain assayed) is Sit4 dependent, whereas long-term starvation (>3–4 hr), correlating with cells arresting in G1, is Sit4 independent (Tate *et al.* 2013). Gln3-Myc^{13} is distributed more or less equally in all three scoring categories (cytoplasmic, nuclear-cytoplasmic, nuclear) in Sit4-dependent, short-term nitrogen starvation; whereas in long-term starvation, Gln3-Myc^{13} becomes completely nuclear (Tate *et al.* 2013).

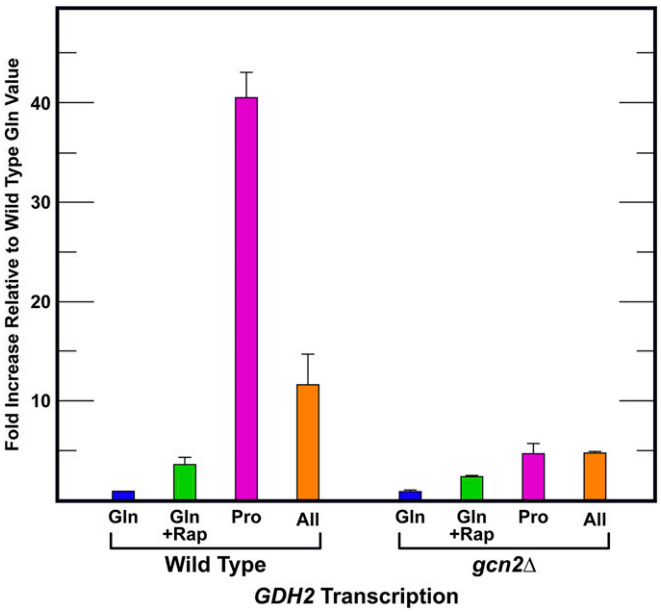

Figure 3 Gcn2 is required for NCR-sensitive *GDH2* gene expression when cells are cultured with derepressive nitrogen sources. *GDH2* expression was measured in wild-type (BY4742) and *gcn2*Δ cells using qRT-PCR provided with glutamine (Gln), proline (Pro), or allantoin (All) as sole nitrogen source. Where indicated, glutamine-grown cells were treated with rapamycin. Total RNA was collected and analyzed as described in *Materials and Methods*. +Rap, addition of rapamycin.

Short- and long-term nitrogen starvation elicited the expected Gln3 behavior cited above in wild-type cells, *i.e.*, Gln3-Myc^{13} localization was equally distributed in the three scoring categories between 0.5 and 3 hr of starvation, and thereafter, became highly nuclear (Figure 4A and Figure 5A). In *gcn2*Δ, the Gln3-Myc^{13} response to short-term nitrogen starvation was unaffected and indistinguishable from wild type (Figure 4B). However, substantial Gln3-Myc^{13} relocation to the nucleus observed between 4 and 6 hr in the wild type did not occur in the mutant, suggesting at face value that Gcn2 was required for long-term nitrogen starvation. It is important to note, however, that *gcn2*Δ grew more slowly than wild type. Therefore, it was possible that the time needed for long-term starvation to occur correspondingly increased. To assess this possibility, we repeated the experiment tracking the bud index of the cultures to ascertain the timing of G1 arrest-correlated, long-term starvation. Wild-type cells behaved as in Figure 4A with Gln3-Myc^{13} becoming substantially nuclear beginning at 3 hr in concert with the increased number of unbudded cells (Figure 5, A and C). The overall profile of unbudded cell formation in *gcn2*Δ was similar to wild type, but was shifted somewhat to longer times (Figure 5C). Increased nuclear Gln3-Myc^{13} localization also occurred in the *gcn2*Δ mutant, but was also slowed relative to wild type, substantially increasing only at 8 hr (Figure 5B). Gln3-Myc^{13} did not quite achieve the same high nuclear levels as wild type. Together these data suggested that Gcn2 activity was not required for the response of Gln3 localization

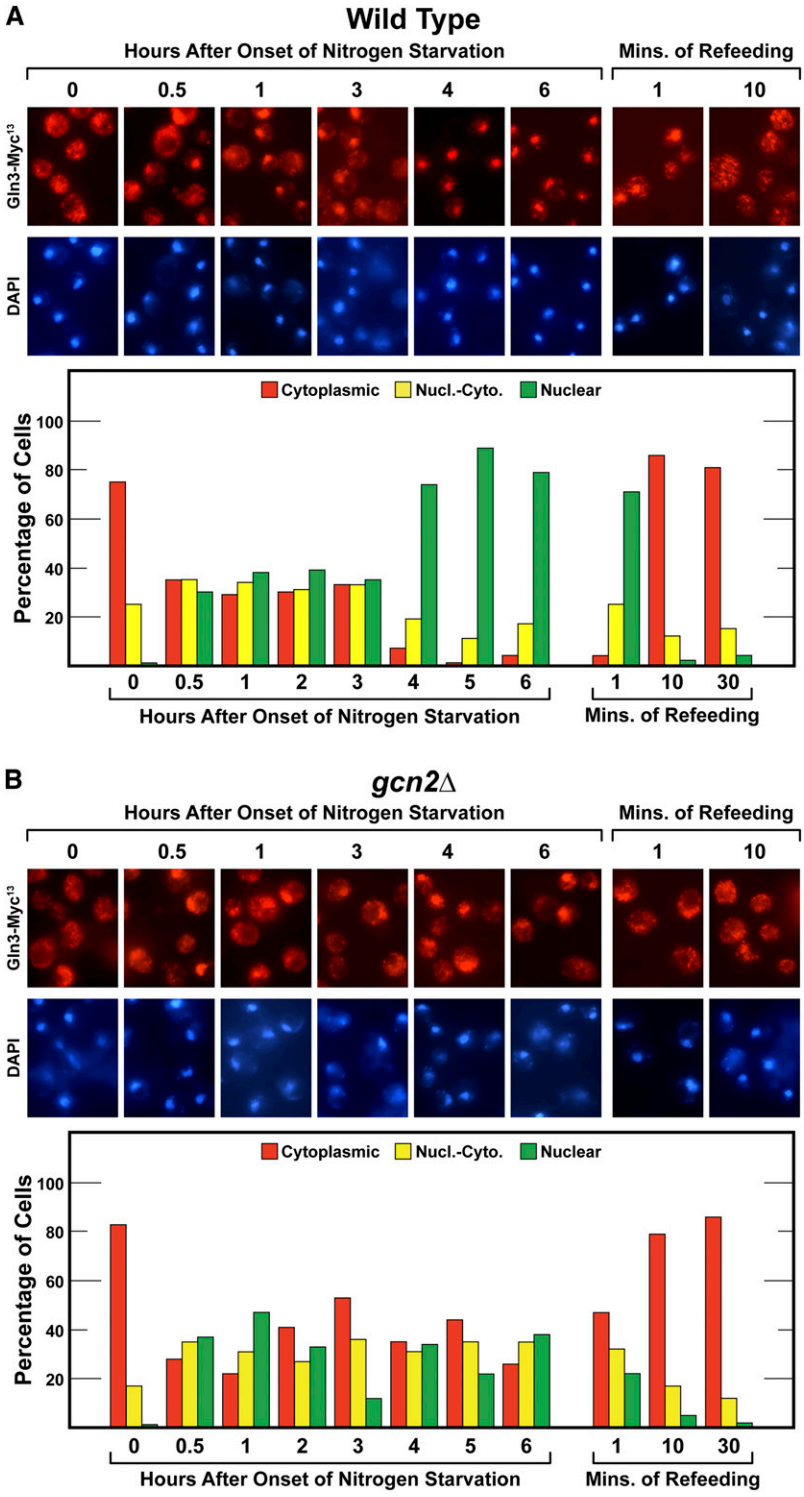

Figure 4 The effects of Gcn2 abolishment on Gln3-Myc^{13} localization in response to short- and long-term nitrogen starvation. (A) Wild-type (BY4742) and (B) *gcn2*Δ cells were grown to $A_{600\ nm}$ = 0.5 in YNB-glutamine medium. They were then transferred (by filtration) to nitrogen-free YNB medium and sampled as indicated for 6 hr. At that time glutamine (0.1%) was added to the culture and sampling continued for 30 min. Gln3-Myc^{13} was visualized and scored as described in *Materials and Methods*. Nucl.-Cyto., nuclear-cytoplasmic.

to short-term or long-term nitrogen starvation. The long-term nitrogen starvation results correlated well with the inability of *gcn2*Δ to affect the Gln3 response to Msx treatment, further attesting to the specificity of the *gcn2*Δ phenotype. It is also noteworthy that Gcn2 was not required for either steady-state cytoplasmic Gln3-Myc^{13} sequestration in glutamine-grown cells (Figure 4B, zero time point), or short-term Gln3-Myc^{13} relocation to the cytoplasm following addition of glutamine to previously starved cells (Figure 4B, 1 and 10 min time points).

ure2Δ is epistatic to gcn2Δ for Gln3-Myc^{13} localization

The dramatic effects of abolishing Gcn2 on Gln3-Myc^{13} localization and *GDH2* transcription prompted the question of whether it was functioning upstream or downstream of Ure2 in the nitrogen-responsive regulatory cascade. Since

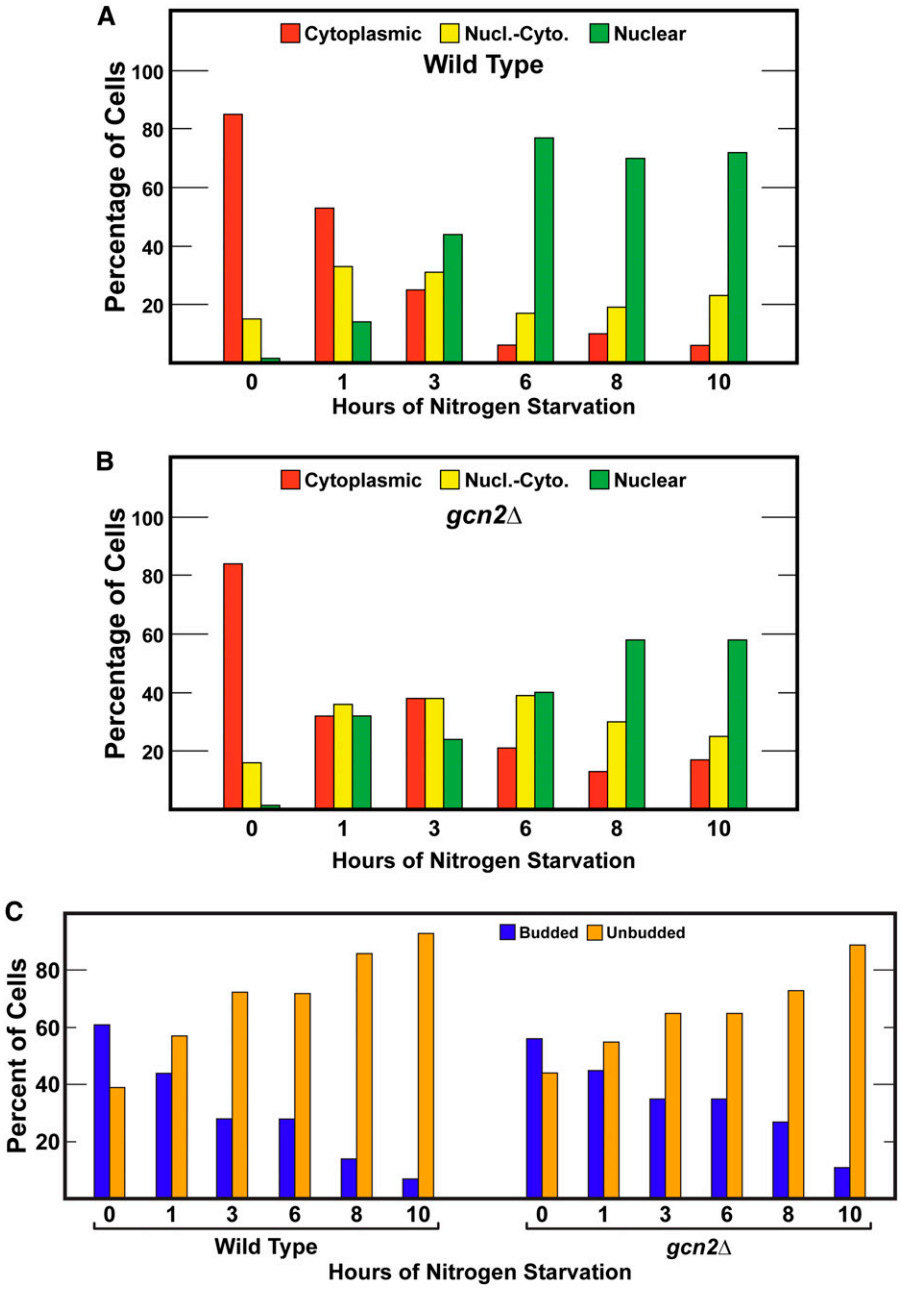

Figure 5 The effects of Gcn2 abolishment on budding and Gln3-Myc[13] localization in response to long-term nitrogen starvation. (A) Wild-type (BY4742) and (B) *gcn2*Δ cells were grown to $A_{600\ nm}$ = 0.5 in YNB-glutamine medium. They were then transferred (by filtration) to nitrogen-free YNB medium and sampled as indicated for 10 hr. Gln3-Myc[13] was visualized and scored as described in *Materials and Methods*. The extent of cell budding (C) was scored in 200 or more cells per determination. Nucl.-Cyto., nuclear-cytoplasmic.

Gln3-Myc[13] is highly nuclear in *ure2*Δ and highly cytoplasmic in *gcn2*Δ, we approached the question by determining the epistatic relationship of the two deletions. To this end, we constructed and validated a *gcn2*Δ,*ure2*Δ double mutant as described in *Materials and Methods*.

On analyzing Gln3-Myc[13] localization we found that Gln3-Myc[13] in wild type, *ure2*Δ, and *gcn2*Δ yielded the expected results: (i) a typical NCR-sensitive response in wild type, cytoplasmic, and nuclear in asparagine *vs.* proline media, respectively; (ii) predominantly nuclear in *ure2*Δ; and (iii) predominantly cytoplasmic in *gcn2*Δ, irrespective of the nitrogen source (Figure 6A). In the *gcn2*Δ*ure2*Δ double mutant, Gln3-Myc[13] was again nearly all nuclear; indicating that *ure2*Δ was epistatic to *gcn2*Δ and therefore Gcn2 was likely functioning upstream of Ure2 (Figure 6A).

To further test this conclusion, we measured *GDH2* gene expression (Figure 6B). As expected, *GDH2* levels were NCR sensitive in wild-type cultures with expression much higher in proline than glutamine medium. Responses in the *gcn2*Δ and *ure2*Δ mutants were again opposite one another, being very low in *gcn2*Δ and higher than wild type in *ure2*Δ. In the *gcn2*Δ,*ure2*Δ double mutant, *GDH2* expression was the same as wild-type derepressed levels, positively correlating with the conclusions reached by measuring Gln3-Myc[13] localization.

It is reasonable to query why relative *GDH2* expression levels in this experiment were lower than those observed in Figure 3.

The reason is that *GDH2* expression in the glutamine-grown cells of this experiment were somewhat higher than in Figure 3, thereby depressing the fold increase observed (note that the level in glutamine medium is defined as 1.0). This occurred because all of the strains in this experiment were transformed with Gln3-Myc^{13} to correlate with data from Figure 6A. Therefore, these strains possessed two copies of the *GLN3* gene which accounted for the higher expression level in glutamine-grown cells. Note that wild-type *GDH2* expression in Figure 6B was the same as that observed in Rai *et al.* (2015).

Components of Gln3 regulation affected by deletion of GCN2

As noted in the Introduction, particular Gln3 residue substitutions adversely affect specific modes of Gln3 regulation. These mutants were previously used to demonstrate that multiple regulatory pathways cumulatively control Gln3 localization (Rai *et al.* 2013, 2014, 2016). Therefore, we wanted to ascertain how loss of Gcn2 would affect Gln3-Myc^{13} localization in each of these mutants and whether Gcn2 acted cumulatively with them. To that end, wild-type and *gcn2*Δ cells were transformed with a wild type or one of four mutant plasmids and the intracellular distribution of Gln3-Myc^{13} determined in proline-grown cells where mTorC1 is least active.

Gln3-Myc^{13} was almost exclusively nuclear in a wild-type transformant containing wild-type Gln3-Myc^{13} (pRR536), and became largely cytoplasmic in *gcn2*Δ (Figure 7). Gln3 was again mostly nuclear when the wild-type recipient (BY4742) was transformed with pRR680, in which Gln3 cannot be putatively phosphorylated because of serine to alanine substitutions (Rai *et al.* 2016). In contrast, when -*gcn2*Δ was used as the transformation recipient, Gln3-Myc^{13} was almost equally distributed in each of the three scoring categories (Figure 7). This phenotype has been repeatedly observed following the loss of one mode of Gln3 regulation (Rai *et al.* 2013, 2014, 2016) and is consistent with Gcn2 being responsible for half of the nuclear localization observed in wild type cells, the remaining half depending on the Gln3 residues substituted in pRR680. Results identical to those with pRR680 were also observed with pRR850, in which the Gln3-mTor1 interaction is abolished (Rai *et al.* 2013). Again, Gcn2 was required for full nuclear Gln3-Myc^{13} localization. A parallel experiment was then performed with pRR1045 and pRR1194. Substitutions in pRR1045 and pRR1194 are situated at N- and C-terminals, respectively, of the domain required for Gln3 relocation to the nucleus when cells are treated with rapamycin. Either of these substitutions abolishes the Gln3 response to rapamycin (Rai *et al.* 2014). In both cases, Gln3-Myc^{13} was no longer exclusively nuclear in the wild-type recipient, but rather equally distributed in the three scoring categories as observed when pRR850 and pRR680 were transformed into *gcn2*Δ (Figure 7). In other words, half of Gln3's ability to localize to the nucleus was lost in the wild-type recipient due to abolishment of the Gln3 site required for a response to treating cells with rapamycin. The remaining half of nuclear Gln3 localization was then abolished when either pRR1045 or pRR1194 was transformed into *gcn2*Δ cells, resulting in Gln3-Myc^{13} being localized almost entirely in the cytoplasm (Figure 7). Therefore, loss of Gln3's ability to respond to rapamycin together with abolishment of Gcn2 cumulatively eliminated nuclear Gln3-Myc^{13} localization.

The uptake and assimilation of ammonia, like that of proline, requires NCR-sensitive transcription, *e.g.*, of the *MEP* permease and *GLN1* glutamine synthetase genes. As with proline, nuclear Gln3-Myc^{13} localization was abolished in ammonia-grown *gcn2*Δ cells (Figure 1B). Therefore, we grew wild-type and *gcn2*Δ transformants containing pRR680, pRR850, or pRR1045 in YNB-ammonia medium and measured Gln3-Myc^{13}. The outcomes of those measurements exhibited similar profiles to those obtained with proline-grown cells in Figure 7 (data not shown), extending the correlation between Gcn2 function and NCR observed in Figure 1 and Figure 2. Together the data argued that Gcn2 functioned as one of the multiple modes of regulation to control nitrogen-responsive Gln3 localization.

Nuclear Gln3-Myc^{13} localization requires Gcn2-regulated Gcn4 activity

Having established participation of the metabolite-proximal global regulator, Gcn2, in Gln3 localization and function, our next objective was to begin trying to understand how that regulation was achieved. The most often observed mechanism of Gcn2-dependent regulation is via its upregulation of Gcn4 translation, a major transcriptional activator responsible for Gcn2-dependent expression of 100s of genes and in particular those required for amino acid biosynthesis. To test whether or not Gcn4 was participating in Gcn2-mediated Gln3 regulation, we obtained a Gcn4 deletion and assayed Gln3-Myc^{13} localization in response to our normal range of conditions. The first thing we noticed was that *gcn4*Δ grew more slowly than *gcn2*Δ, indicating that residual Gcn4 activity present in *gcn2*Δ was an important determinant in the growth phenotype. The Gln3-Myc^{13} responses in *gcn4*Δ cultured with a range of poor nitrogen sources were the same as those observed with *gcn2*Δ (Figure 8A). Similarly, equivalent Gln3-Myc^{13} localization responses were also observed in *gcn2*Δ and *gcn4*Δ cells subjected to short- and long-term nitrogen starvation (Figure 8, B–D). These data indicated that Gcn2-dependent regulation of Gln3 localization required Gcn4. Importantly, they also showed that the function lost in *gcn4*Δ could not be fulfilled by the basal levels of Gcn4 that are present in *gcn2*Δ.

Gln3-Myc^{13} is dephosphorylated in gcn2Δ and gcn4Δ mutants

Although open questions remain (Tate *et al.* 2009; Feller *et al.* 2013), many models of mTorC1-mediated Gln3 regulation envision Gln3 to be dephosphorylated, thereby bringing about its dissociation from the Gln3-Ure2 complex and thus localization to the nucleus (Beck and Hall 1999; Bertram *et al.* 2000; Carvalho and Zheng 2003). Therefore, it was

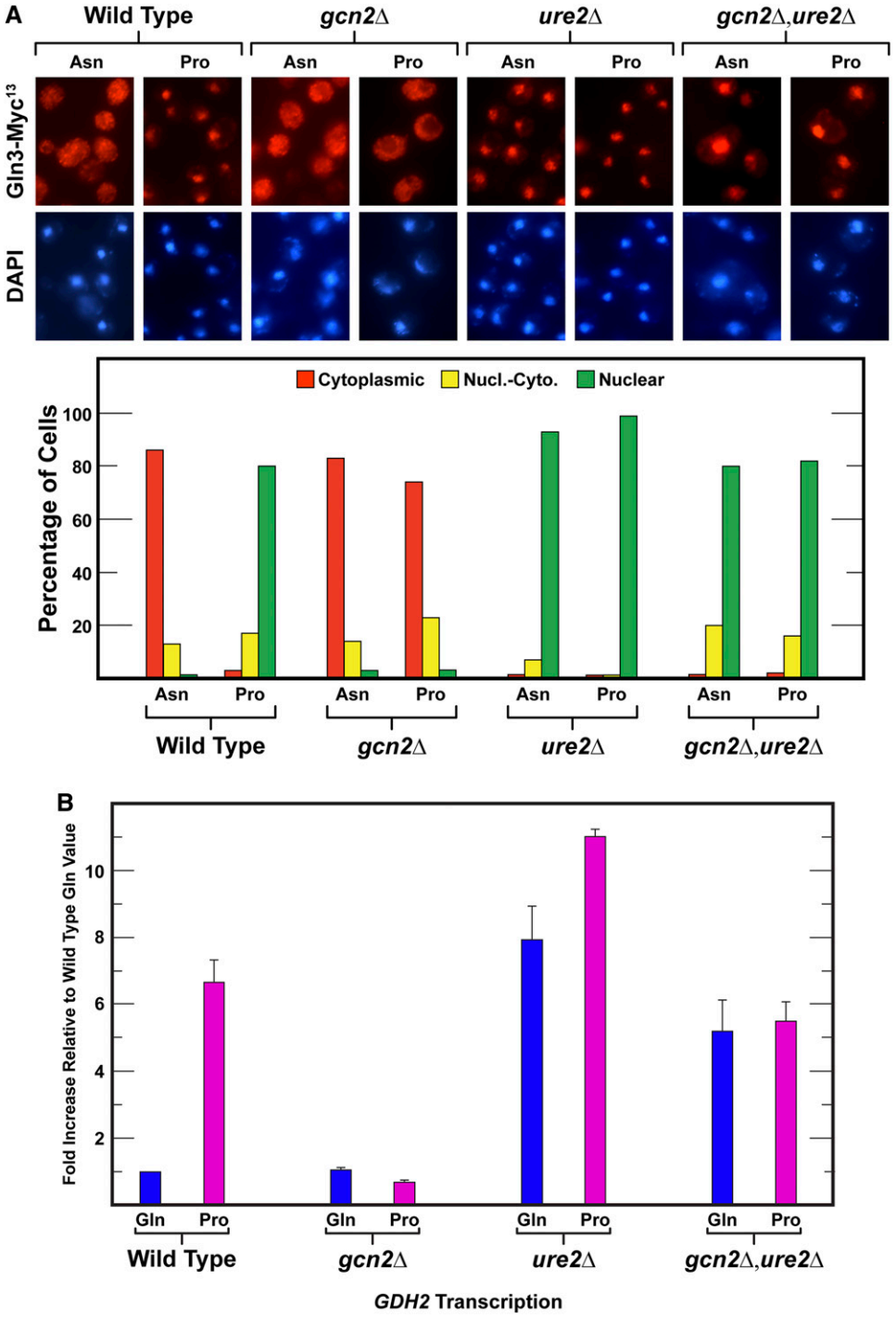

Figure 6 *ure2*Δ is epistatic to *gcn2*Δ. Wild type (BY4742), *gcn2*Δ, *ure2*Δ (RR259), and *gcn2*Δ*ure2*Δ (JT11) mutants were cultured in YNB-glutamine (Gln), -asparagine (Asn) or -proline (Pro) medium. (A) Intracellular Gln3-Myc^{13} localization was followed in the various mutants grown in asparagine or proline medium as described in Figure 1. (B) Total RNA was harvested as described in *Materials and Methods* and subjected to qRT-PCR analysis using a *GDH2* probe as described in Figure 3. Nucl.-Cyto., nuclear-cytoplasmic.

appropriate to ascertain whether Gln3-Myc^{13} phosphorylation levels, *i.e.*, its electrophoretic mobility in Western blots, were altered in *gcn2*Δ and *gcn4*Δ mutants. To this end, we prepared extracts of glutamine-, ammonia-, or proline-grown wild-type *vs.* *gcn2*Δ cells. Gln3-Myc^{13} mobility increased in glutamine-, ammonia- and proline-grown *gcn2*Δ cells relative to wild type (Figure 9A). The increased mobility was most apparent in the ammonia- and proline-grown cells where the slowest mobility species all but disappeared (Figure 9A, lanes 1–4). Such increased Gln3 mobility has repeatedly been shown to result from decreased phosphorylation (Beck and Hall 1999; Bertram *et al.* 2000; Cox *et al.* 2004a,b; Tate and Cooper 2007). In other words, the presence of Gcn2 increased Gln3-Myc^{13} phosphorylation levels. This prompted us to query whether Gln3-Myc^{13} dephosphorylation levels would increase even further in rapamycin-treated *gcn2*Δ cells.

We addressed this question by comparing Gln3-Myc^{13} mobilities in wild-type and *gcn2*Δ cells treated with rapamycin. The mobility profiles of Gln3-Myc^{13} derived from glutamine-grown, rapamycin-treated wild-type and *gcn2*Δ cells were

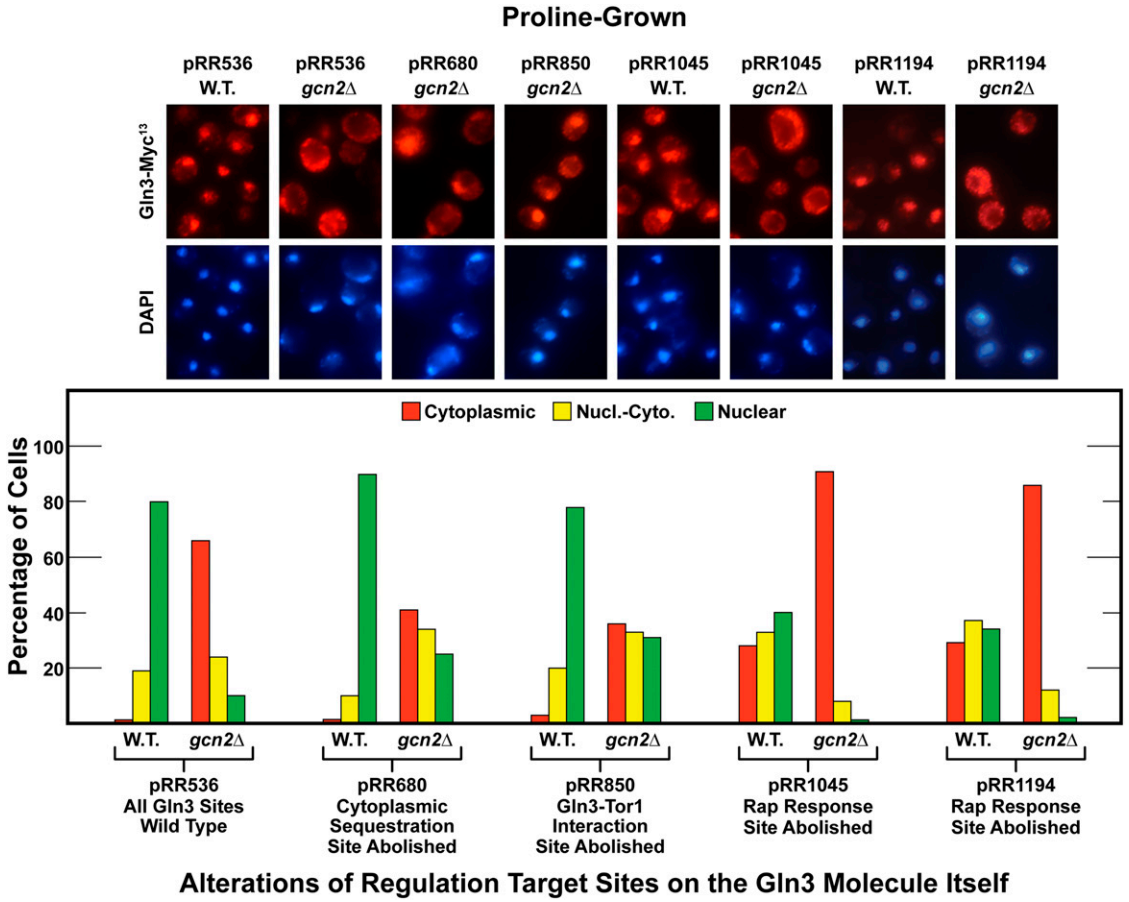

Figure 7 Gcn2 and mTorC1 are coregulators of intracellular Gln3-Myc^{13} regulation. Wild type (BY4742) and *gcn2*Δ strains were transformed with wild type (pRR536) and *gln3* substitution mutant plasmids pRR680, pRR850, pRR1045, and pRR1194. The transformants were then grown in YNB-proline medium and Gln3-Myc^{13} intracellular localization assayed. The format and presentation of the experimental data were as described in Figure 1. Nucl.-Cyto., nuclear-cytoplasmic; W.T., wild type.

indistinguishable (Figure 9B; lanes 1, 2, 6, and 7). The loss of Gcn2 had no demonstrable effect on rapamycin-mediated Gln3-Myc^{13} dephosphorylation. Recall that loss of Gcn2 also had no effect on Gln3-Myc^{13} localization in glutamine-grown, rapamycin-treated cells (Figure 1). Therefore, we repeated the experiment, but this time used ammonia-grown cells where the loss of Gcn2 does have a marked effect on both Gln3-Myc^{13} localization and mobility. Similar to what occurred earlier, rapamycin treatment of ammonia-grown wild-type and *gcn2*Δ cells exhibited electrophoretic mobility profiles that were indistinguishable (Figure 9C, lanes 2–5). Similarly, the electrophoretic mobility profiles in Msx-treated wild-type and *gcn2*Δ cells were also indistinguishable. The lack of responses to rapamycin or Msx treatment again supports the specificity of the *gcn2*Δ phenotype.

To evaluate the potential participation of Gcn4 in Gln3-Myc^{13} dephosphorylation, we prepared a set of Western blots analogous to those in Figure 9, A–C, using extracts from *gcn4*Δ. Gln3-Myc^{13} mobility increased under the same conditions as it had in *gcn2*Δ (Figure 9, D–F). These results indicated that Gln3-Myc^{13} dephosphorylation was Gcn4 dependent. Since Gcn4 is a transcription activator rather than a kinase or phosphatase, the protein directly responsible for Gln3-Myc^{13} dephosphorylation is situated downstream of Gcn4 in the GAAC cascade.

Nuclear Gat1-Myc^{13} localization is also Gcn2 dependent

Gln3 and Gat1 share some, but not all, regulatory characteristics in common (Georis *et al.* 2008, 2011). Therefore, it was of interest to ascertain whether or not Gcn2 played a role in nuclear Gat1-Myc^{13} localization as well. In this context, it is important to recall that Gat1 localization is not nearly as NCR sensitive as Gln3 (Georis *et al.* 2008, 2011). We assayed the Gat1-Myc^{13} localization responses in wild-type and *gcn2*Δ cells and found the overall responses were similar to those obtained with Gln3 (Figure 10, compare with Figure 1).

Nuclear Gln3-Myc^{13} localization is abolished in a bmh1Δ,bmh2Δ double mutant

The preceding data showing that Gln3-Myc^{13} phosphorylation and nuclear localization both decreased in the *gcn2*Δ and *gcn4*Δ mutants prompted us to query whether the phosphoprotein binding 14-3-3 proteins, Bmh1/2, participated in Gln3

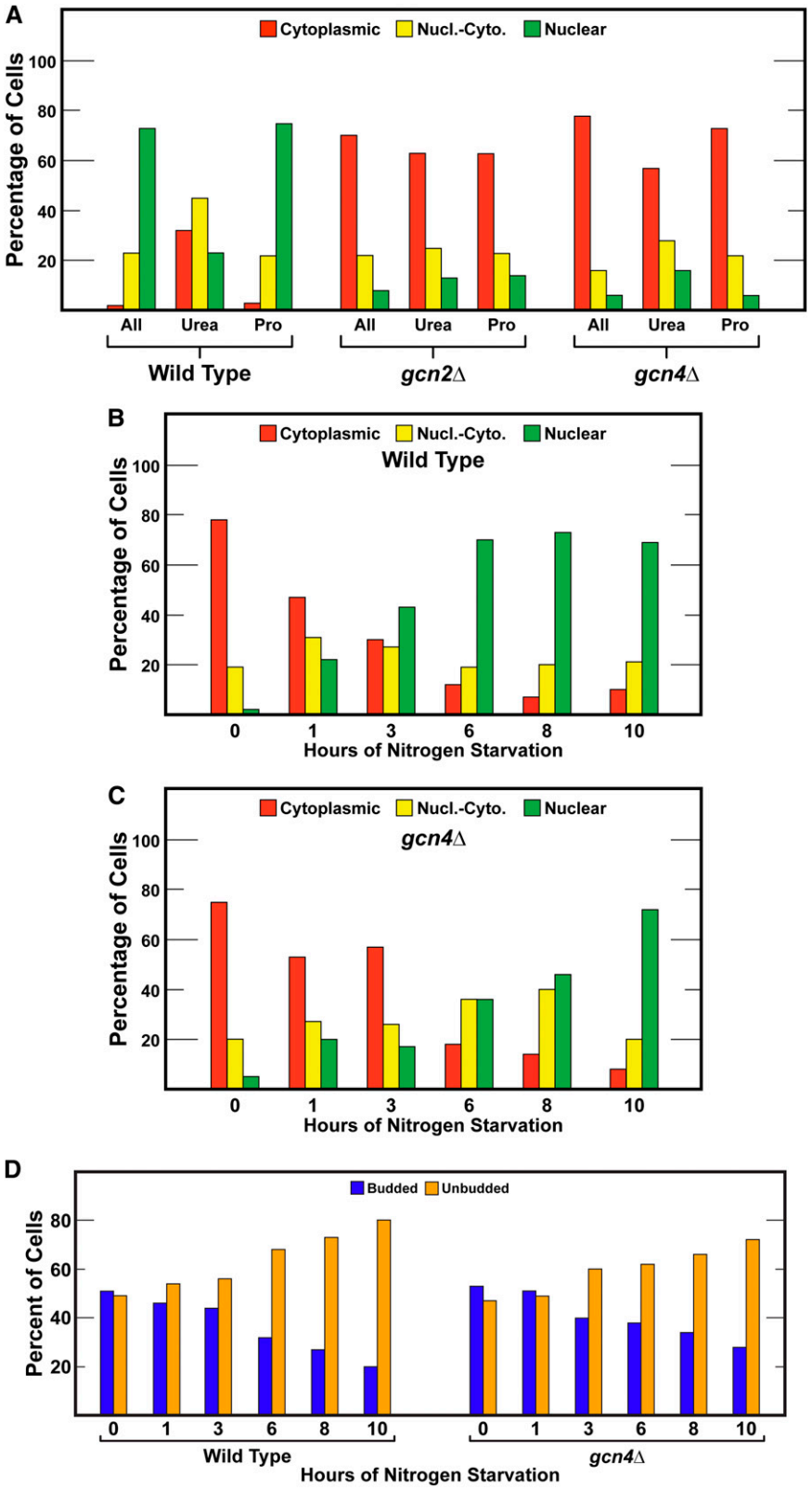

Figure 8 (A) Gcn4 is required for nuclear Gln3-Myc[13] localization in response to growth with nitrogen sources whose use requires NCR-sensitive transcription. Gln3-Myc[13] localization was measured in wild-type (BY4742), *gcn2*Δ, and *gcn4*Δ cells cultured in YNB-minimal medium provided with allantoin (All), urea, or proline (Pro) as nitrogen source. The format and presentation of the experimental data were as described in Figure 1. (B and C) Effects of Gcn4 abolishment on Gln3-Myc[13] localization and cell budding (D) during nitrogen starvation. The format of the experiment and presentation of the data are as described in Figure 5. Nucl.-Cyto., nuclear-cytoplasmic.

localization and function. This was not as far-fetched a question as it might seem because Bmh2 has been reported to interact with Gln3 in genome-wide association liquid chromatography tandem-mass spectrometry (MS) analyses (Kakiuchi *et al.* 2007). Therefore, we assayed the expression of three NCR-sensitive genes, *GDH2*, *DAL80*, and *DAL5* in wild-type and *bmh1*Δ,*bmh2*Δ double mutant cells (Figure 11). As previously shown, *GDH2*, whose expression is highly Gln3 dependent

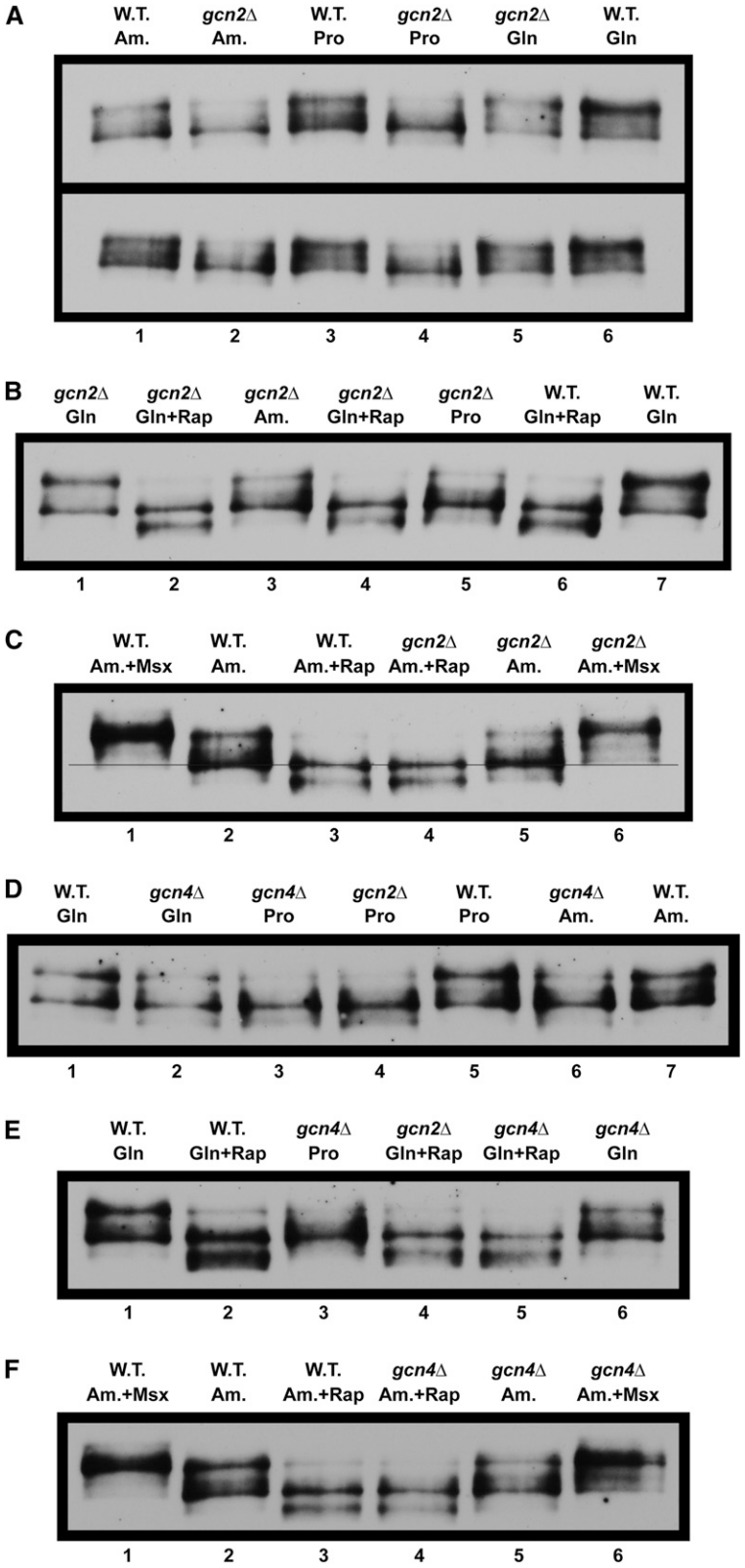

Figure 9 Gln3-Myc[13] phosphorylation levels decrease when Gcn2 (Panels A-C) or Gcn4 (Panels D-F) is abolished. Cell-free extracts were prepared from wild-type (BY4742), *gcn2*Δ, or *gcn4*Δ cultures grown in YNB-ammonia (Am.), -proline (Pro), or -glutamine (Gln). Rapamycin (+Rap) or Msx (+Msx) were added as indicated. Proteins in the extracts were then resolved using SDS-PAGE and Western blots prepared and visualized as described in *Materials and Methods*. W.T., wild type.

(Georis *et al.* 2011), was highly NCR sensitive in wild-type cells; being expressed only in derepressive proline medium (Figure 11A, lanes 1–5). In contrast, *GDH2* expression was almost completely abolished in a *bmh1*Δ,*bmh2*Δ double mutant (Figure 11A, lanes 6–10). This and the following experiments with the *bmh1*Δ,*bmh2*Δ mutant were performed in a Σ1278b background, because Σ1278b is one of the very few strains where a *bmh1*Δ,*bmh2*Δ double mutant grows (Roberts *et al.* 1997).

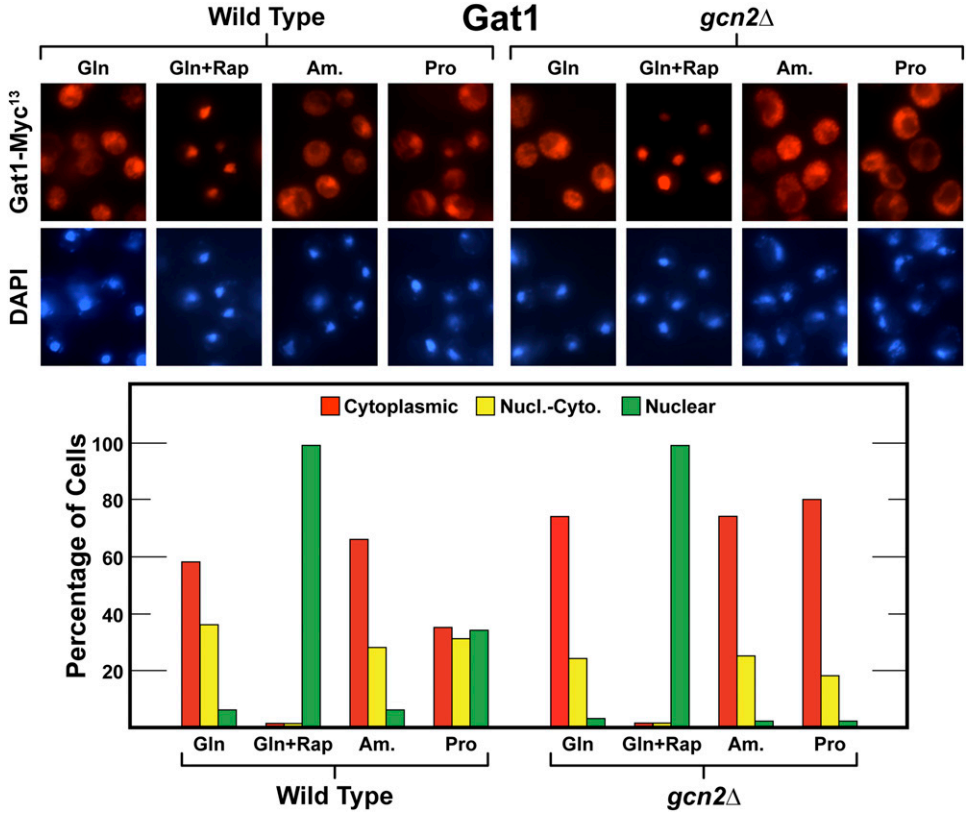

Figure 10 Gcn2 is required for nuclear Gat1-Myc[13] localization in response to growth with nitrogen sources whose use requires NCR-sensitive transcription. Cells were cultured in YNB-glutamine (Gln), -ammonia (Am.), or -proline (Pro) medium. Rapamycin (+Rap) was added where indicated. The format and data presentation were as described in Figure 1. Nucl.-Cyto., nuclear-cytoplasmic.

Similar results were obtained with the NCR-sensitive *DAL80* and *DAL5* genes (Figure 11, B and C). Note that their decreased NCR sensitivity (expression with urea and serine in addition to proline) correlates with the strong participation of Gat1 in their expression (Coffman *et al.* 1996, 1997; Cunningham *et al.* 2000a,b). As with *GDH2*, their expression was abolished in *bmh1*Δ,*bmh2*Δ. Retrograde *CIT2* expression was abolished in wild-type glutamine- and proline-grown cells and highly expressed when ammonia was provided as nitrogen source, as previously reported (Tate and Cooper 2003) (Figure 11D, lanes 1–5). In contrast, *CIT2* was expressed constitutively in *bmh1*Δ,*bmh2*Δ in agreement with Liu *et al.* (2003, 2005) (Figure 11D, lanes 6–10).

Next we determined whether the response of NCR-sensitive transcription to rapamycin treatment was adversely affected by the loss of Bmh1/2. As shown in Figure 12, the rapamycin response was also drastically diminished, but was not absolutely abolished in *bmh1*Δ,*bmh2*Δ. It is important to note that the adverse effects of *bmh1*Δ,*bmh2*Δ diminishes as the nitrogen source employed becomes more derepressive. In this strain, the strength of repression order is glutamine > ammonia > urea > proline (Cooper 1982). Yet rapamycin is envisioned to efficiently inhibit mTorC1 downstream of the metabolic signal controlling its activity, making this yet another demonstration of the multipartite regulation of Gln3 function.

bmh1Δ,bmh2Δ is epistatic to ure2Δ

Our next goal was to determine whether Bmh1/2 participated in Gln3 regulation upstream or downstream of Ure2. To this end we performed an epistasis test between *bmh1*Δ,*bmh2*Δ and *ure2*Δ. *DAL5* and *DAL80* expression was equally robust in glutamine-, ammonia- or proline-grown *ure2*Δ cells, as expected (Figure 13, A and B, lanes 1–3). In sharp contrast, it was all but undetectable in the *bmh1*Δ,*bmh2*Δ mutant (Figure 13, A and B, lanes 4–6). Strikingly, NCR-sensitive *DAL5* and *DAL80* expression was undetectable in *ure2*Δ,*bmh1*Δ, *bmh2*Δ cells, indicating that *bmh1*Δ,*bmh2*Δ was epistatic to *ure2*Δ. This suggested that Bmh1/2 function downstream of Ure2 in the Gln3 regulatory cascade.

Bmh1/2 are required for nuclear Gln3-GFP localization

To ascertain whether the requirements for Gln3 localization correlated with NCR-sensitive transcription, we compared its localization in ammonia-grown, rapamycin- or Msx-treated cells (Figure 14 and Figure 15, respectively). This routine experiment turned out to be much more challenging than expected due to a surprising phenotype of the *bmh1*Δ,*bmh2*Δ mutations. *bmh1*Δ,*bmh2*Δ cells form pseudohyphal-like cell chains similar to those seen in the minor glutamine $tRNA_{CUG}$ *sup70-65* mutant, making it more difficult to determine Gln3-Myc[13] localization (compare Figure 14 and Figure 15 with figure 5 and figure 6 in Tate *et al.* 2015b). First, as occurred earlier with *sup70-65*, the *bmh1*Δ,*bmh2*Δ cells were too fragile to employ our standard indirect immunofluorescence methodology (Tate *et al.* 2015b). We thus resorted to the use of Gln3-GFP. Unfortunately, this method does not permit as large a number of cells to be scored, because unconcentrated, growing cultures are being imaged. Further, it is also

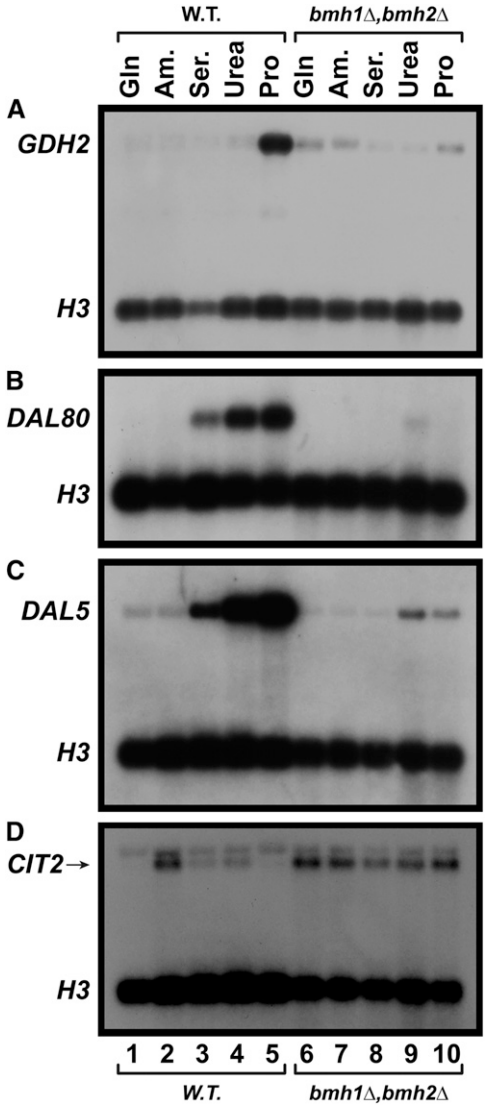

Figure 11 NCR-sensitive gene expression is abolished in a *bmh1*Δ, *bmh2*Δ mutant, whereas retrograde gene expression becomes constitutive. Wild-type (10560-2B) and *bmh1*Δ,*bmh2*Δ (RRY1216) cultures were grown to $A_{600\ nm}$ = 0.5 in YNB medium containing the indicated nitrogen source: glutamine (Gln), ammonia (Am.), serine (Ser.), urea, or proline (Pro). Total RNA was then isolated and Northern blots prepared as described in *Materials and Methods*. Blots were probed for NCR-sensitive [(A) *GDH2*, (B) *DAL80*, or (C) *DAL5* probes] or retrograde [(D) *CIT2*] gene expression. H3 was used as the loading control. W.T., wild type.

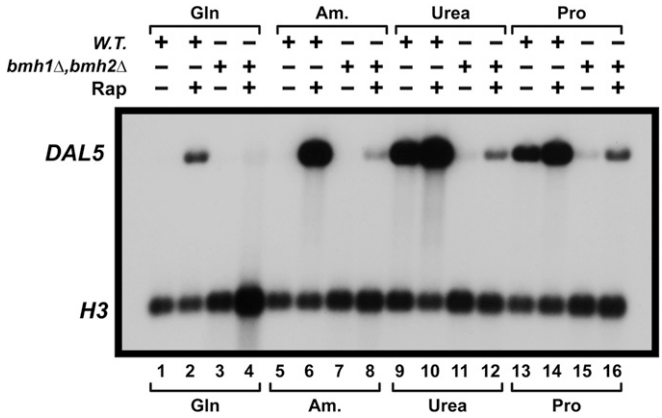

Figure 12 Rapamycin-elicited, NCR-sensitive gene expression is abolished in *bmh1*Δ,*bmh2*Δ. Wild type (10560-2B) and *bmh1*Δ,*bmh2*Δ (RRY1216) were cultured in YNB medium containing the indicated nitrogen source. The cultures were then treated with 200 ng/ml rapamycin. Northern blots were prepared as described in *Materials and Methods*. Am., ammonia; Gln, glutamine; Pro, proline; Rap, rapamycin; W.T., wild type.

not possible to confidently distinguish cells where Gln3-GFP is nuclear from those where it is nuclear-cytoplasmic because of the significant background fluorescence in the unaltered images we use for scoring (Tate *et al.* 2015b). As a result, the nuclear and nuclear-cytoplasmic categories are combined as nuclear-cytoplasmic. Hence point-to-point variation of the data in a time-course experiment is a bit higher than if Gln3-Myc^{13} were being assayed.

These difficulties notwithstanding, Gln3-GFP quickly (within 6 min or more) relocated from being cytoplasmic in almost 100% of the wild-type cells to becoming nuclear-cytoplasmic in ~70–80% following rapamycin treatment (Figure 14A). In contrast, similar Gln3-GFP relocation largely failed to occur in the *bmh1*Δ,*bmh2*Δ cells. Gln3-GFP continued to reside in the cytoplasm of ~70–80% of the cells following the addition of rapamycin (Figure 14B). Although Gln3-GFP partitioning in the *bmh1*Δ,*bmh2*Δ cells was not as tight as observed in the transcription experiments, a positive correlation is clearly present.

We then repeated the experiment using Msx in place of rapamycin. In wild-type cells, Gln3-GFP relocated from being cytoplasmic in 80–90% of untreated cells to being only 10–20% cytoplasmic once maximal levels of relocation were achieved following the addition of Msx (Figure 15A). When the experiment was performed with Msx-treated *bmh1*Δ, *bmh2*Δ cells, Gln3-GFP was cytoplasmic in nearly 100% of the untreated cells and at most time points did not fall below being 70–80% cytoplasmic (Figure 15B). Although there was greater nuclear Gln3-GFP localization in Msx- than rapamycin-treated cells, it was also decreased in *bmh1*Δ, *bmh2*Δ cells.

Loss of Bmh1,Bmh2 increases Gln3-Myc^{13} mobility in a manner similar to loss of Gcn2

The fact that Bmh1/2 bind to phospho-proteins prompted us to ascertain the effects of abolishing them on Gln3-Myc^{13} phosphorylation. To that end, we prepared Western blots of extracts from ammonia-grown, untreated or rapamycin-treated, wild-type, and *bmh1*Δ,*bmh2*Δ cells. Abolishing Bmh1/2 in untreated cells increased Gln3-Myc^{13} mobility relative to wild type, indicative of Gln3-Myc^{13} hypo-phosphorylation (Figure 16A). Recall that increased Gln3-Myc^{13} mobility also occurred in untreated, ammonia-grown *gcn2*Δ cells (Figure 9A). Treating wild-type cells with rapamycin generated a similar increase in Gln3-Myc^{13} dephosphorylation (Figure 16B). In fact, Gln3-Myc^{13} species exhibited

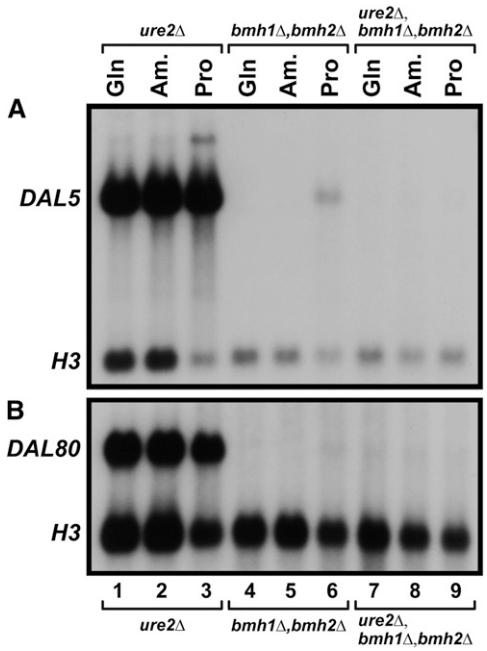

Figure 13 (A and B) *bmh1*Δ,*bmh2*Δ is epistatic to *ure2*Δ. *ure2*Δ (RR114), *bmh1*Δ,*bmh2*Δ (RRY1216), and *ure2*Δ, *bmh1*Δ,*bmh2*Δ (BS0033a) cells were cultured in YNB medium containing the indicated nitrogen sources. Total RNA was then isolated and Northern blots prepared. These blots were probed for NCR-sensitive gene expression with (A) *DAL5* and (B) *DAL80* probes. Am., ammonia; Gln, glutamine; Pro, proline.

indistinguishable electrophoretic mobilities in rapamycin-treated, wild-type, and *bmh1*Δ,*bmh2*Δ cells (Figure 16C). However Gln3-GFP is nuclear in rapamycin-treated wild-type cells, but not in *bmh1*Δ,*bmh2*Δ cells.

Discussion

New regulatory components required for NCR-sensitive Gln3 control

Results presented in this work substantially expand our understanding of GATA factor-mediated, NCR-sensitive regulation by identifying three new important players in the Gln3 nitrogen-responsive cascade: GAAC components, *i.e.*, the Gcn2 protein kinase; the Gcn4 transcription activator; as well as the 14-3-3 phosphoprotein-binding proteins Bmh1/2 (Figure 17A). Epistasis data suggest that Gcn2 functions upstream of Ure2, while Bmh1/2 function downstream of it. Previous data demonstrated that multiple regulatory pathways cumulatively and independently control nitrogen-responsive relocation of Gln3 from the cytoplasm to the nucleus (Rai *et al.* 2016). mTorC1 represents one of these pathways and the data presented in this work lead us to conclude that GAAC via charged tRNA-mediated regulation of Gcn2 is another. Identification of these two metabolite-proximal global regulators as being cumulatively responsible for NCR-sensitive control of Gln3 relocation from the cytoplasm to the nucleus, and the ability to parse their effects using *gln3* amino acid substitution mutants, will significantly facilitate further elucidation of the detailed molecular mechanisms involved.

Participation of GAAC components Gcn2 and Gcn4

gcn2 and *gcn4* mutant responses to a range of growth conditions precisely correlated with those expected when Gln3 is unable to mediate NCR-sensitive transcription or the *GLN3* gene is deleted. Loss of Gcn2 or Gcn4 did not significantly affect growth or Gln3-Myc^{13} localization in repressive nitrogen sources such as glutamine or asparagine where Gln3 is minimally required. In contrast, growth with nitrogen sources that require nuclear Gln3 localization and Gln3-dependent transcription were drastically decreased along with Gln3-Myc^{13} phosphorylation when *GCN2* or *GCN4* were deleted. Positively correlating with these gross growth and phosphorylation responses, nuclear Gln3-Myc^{13} localization and Gln3-mediated, NCR-sensitive transcription were abolished and drastically diminished following the loss of Gcn2. A similar loss of nuclear Gln3-Myc^{13} localization occurred upon deleting *GCN4*. The effects of losing GAAC-mediated Gln3 regulation was not a general, off-target decrease in Gln3 localization. There was high specificity to the effects of deleting *GCN2* or *GCN4* (Figure 17A). Physiological conditions previously demonstrated to be associated with other modes of Gln3 regulation were unaffected by deleting *GCN2* or *GCN4*: (i) rapamycin inhibition of mTorC1, (ii) Msx inhibition of glutamine synthetase, and (iii) long-term nitrogen starvation. This degree of specificity and correlation argues strongly against the *gcn2* and *gcn4* mutant phenotypes we report deriving from indirect, off-target effects of the deletions. It is difficult to see, however, how a transcription activator such as Gcn4 could directly influence intracellular Gln3 localization, leading us to conclude that an unidentified, Gcn2/Gcn4-dependent, Gln3 regulator that acts negatively on Ure2 function remains to be found.

This conclusion is most strongly supported by data obtained with the Gln3 substitution mutants, pRR1045 and pRR1194 (Figure 7). When *GCN2* and Gln3 residues required for rapamycin-elicited nuclear Gln3 localization (Gln3 rapamycin target) are both wild type, as when pRR536 was transformed into wild-type cells, Gln3-Myc^{13} is predominantly nuclear. In contrast, when the Gln3 rapamycin target is abolished but *GCN2* remains wild type, as when pRR1045 or pRR1194 was transformed into wild-type cells, half of the nuclear Gln3-Myc^{13} localization is lost and the characteristic tripartite Gln3-Myc^{13} intracellular distribution is observed. Finally, when both the Gln3 rapamycin target and *GCN2* are abolished, as when pRR1045 or pRR1194 was transformed into *gcn2*Δ cells, the remaining nuclear Gln3-Myc^{13} localization is lost and Gln3-Myc^{13} becomes predominantly cytoplasmic. Thus the outcomes of the rapamycin-inhibiting mTorC1 regulatory pathway and presence of the Gcn2 GAAC pathway are cumulatively responsible for nuclear Gln3 localization in

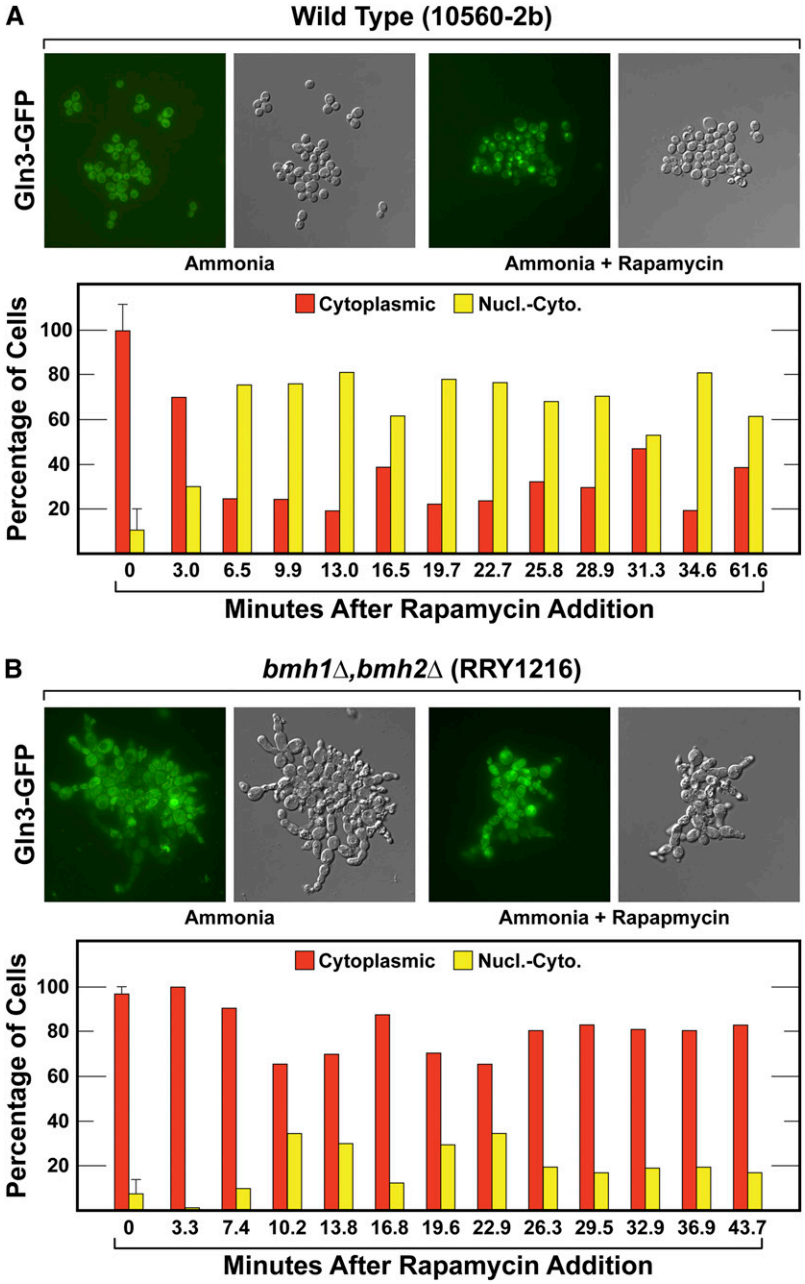

Figure 14 Nuclear Gln3-GFP localization in response to rapamycin treatment requires Bmh1/2. Gln3-GFP (pRS416-GLN3-GFP) transformants of (A) wild-type (10560-2B) and (B) *bmh1*Δ,*bmh2*Δ (RRY1216) cultures were grown in YNB-glutamine medium to a cell density of $A_{600\ nm}$ = 0.5. Six samples (two images each) were collected for the zero time point and then pairs of images were collected thereafter for 60 min following rapamycin treatment. As described in the text, Gln3-GFP localization was scored as either completely cytoplasmic or nuclear-cytoplasmic. Nucl.-Cyto., nuclear-cytoplasmic.

proline-grown cells. The unaffected rapamycin response of Gln3 in *gcn2*Δ (Figure 1) indicates that the rapamycin-sensitive mTorC1- and Gcn2-dependent regulatory pathways are functioning independently.

Opposing mTorC1- and Gcn2/Gcn4-mediated regulation maintains nutrient homeostasis

The effects of nitrogen availability and hence overall amino acid and charged tRNA levels on mTorC1- and Gcn2/Gcn4-mediated control of Gln3 localization is a fascinating example of opposing regulation (Figure 17B). Nitrogen-replete medium elicits opposite effects on these two global regulators but with the same downstream outcomes: High amino acid levels, generated in nitrogen-replete media, minimize the need for NCR-sensitive transcription and, along with charged $tRNA_{Leu}$, activate mTorC1. Activated mTorC1 in turn upregulates protein synthesis initiation and downregulates Gcn2 needed for nuclear Gln3 localization. Additionally, the high levels of charged tRNA in nitrogen excess further downregulate Gcn2 which is required to inactivate protein synthesis initiation and to upregulate nuclear Gln3 localization. Hence, nuclear Gln3 localization fails to occur in nitrogen excess. On the other hand, low amino acid flux, which occurs when scavenging poor nitrogen sources, inactivates mTorC1 and decreases charged tRNA levels, both of which activate Gcn2 and inhibit protein synthesis initiation (Cherkasova and Hinnebusch 2003; Hinnebusch 2005; Staschke *et al.* 2010; Castilho *et al.* 2014; Lageix

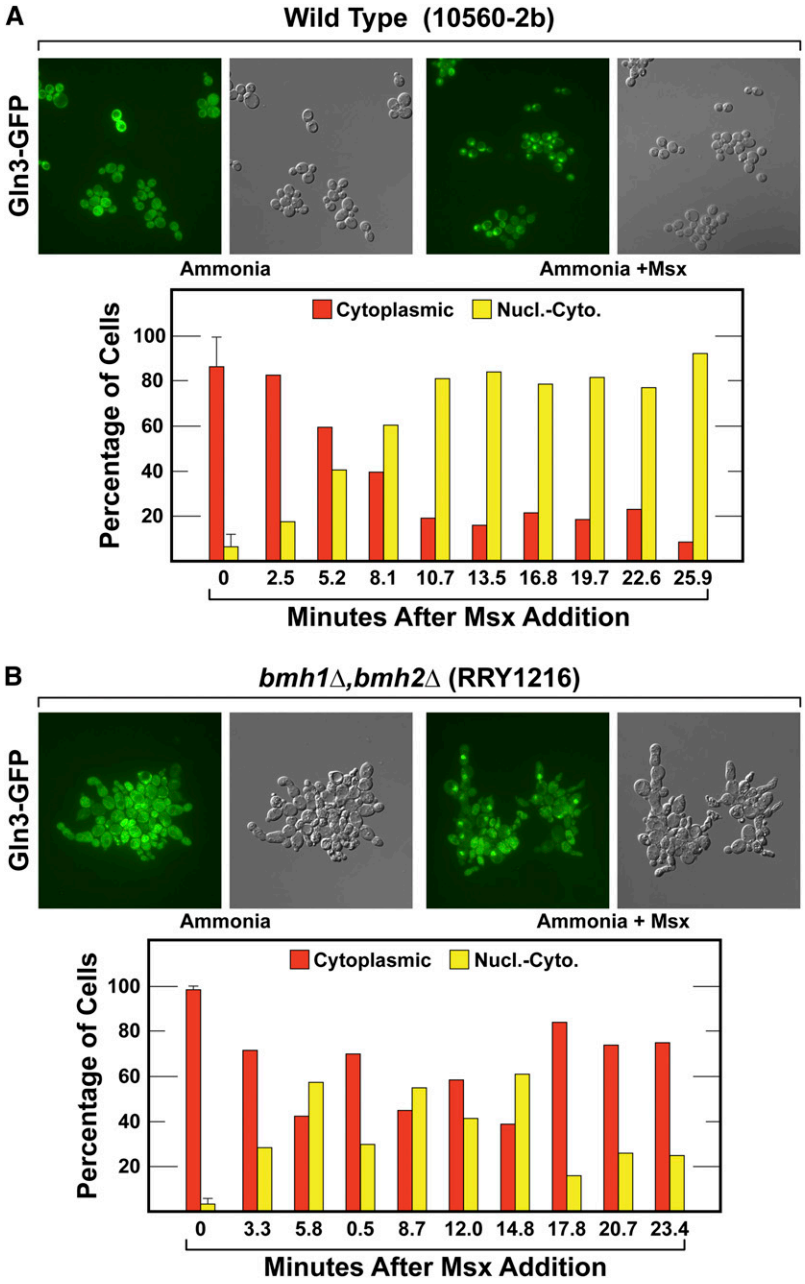

Figure 15 Nuclear Gln3-GFP localization in response to Msx treatment is reduced in *bmh1*Δ,*bmh2*Δ. (A) Wild-type (10560-2b) and (B) *bmh1*Δ,*bhm2*Δ cells (RRY1216). The experiment was performed as described in Figure 14, except that the cells were treated with Msx for ~25 min in place of rapamycin. Nucl.-Cyto., nuclear-cytoplasmic.

et al. 2015; Dever *et al.* 2016). Active Gcn2 upregulates nuclear Gln3 localization, thereby increasing the cell's ability to maintain the supply of nitrogen precursors required for amino acid biosynthesis in an adverse nitrogen environment.

Completing the supply and demand homeostatic circle, the downstream outcomes of Gln3 regulation generate the signals that control both mTorC1 and Gcn2 activities in conditions where the nitrogen supply is limiting. Two major metabolic inputs drive protein synthesis and the signals to which mTorC1 and Gcn2 respond. The internal nitrogen supply derives from vacuolar accumulation of nitrogen-rich compounds (amino acids, allantoin, glutathione, *etc.*) and protein degradation, fed by autophagic import of cytoplasmic components into the vacuole. The external nitrogen supply derives from cytoplasmic nitrogen supplied by the environment via nitrogenous compound transport into the cell and cytoplasmic degradation/interconversion. Both of these inputs are controlled by Gln3. Supporting this conclusion are the following observations: (i) the transcription of the *ATG8* and *ATG14* genes encoding critical components of the autophagic pathway are Gln3- and Gat1-dependent (Kirisako *et al.* 1999; Huang *et al.* 2000; Chan *et al.* 2001); (ii) autophagy occurs at high levels in *ure2*Δ where Gln3/Gat1-activated, NCR-sensitive transcription is constitutive (Noda and Ohsumi 1998); and (iii) transcription of the genes encoding the proteins required for the transport and catabolism of all poor nitrogen sources is NCR-sensitive

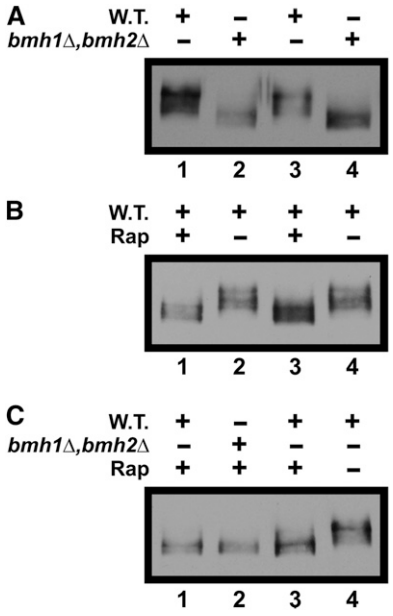

Figure 16 Gln3-Myc[13] phosphorylation decreases in a *bmh1*Δ,*bmh2*Δ mutant. Wild-type (10560-2B, Panels A-C) and *bmh1*Δ,*bmh2*Δ (RRY1216, Panels A and C) cells were cultured to a cell density of $A_{600\ nm}$ = 0.5 in YNB-ammonia medium. Cultures were then treated with 200 ng/ml rapamycin where indicated. Extracts of all cultures were then prepared and subjected to western blot analyses as described in *Materials and Methods*. Rap, rapamycin; W.T., wild type.

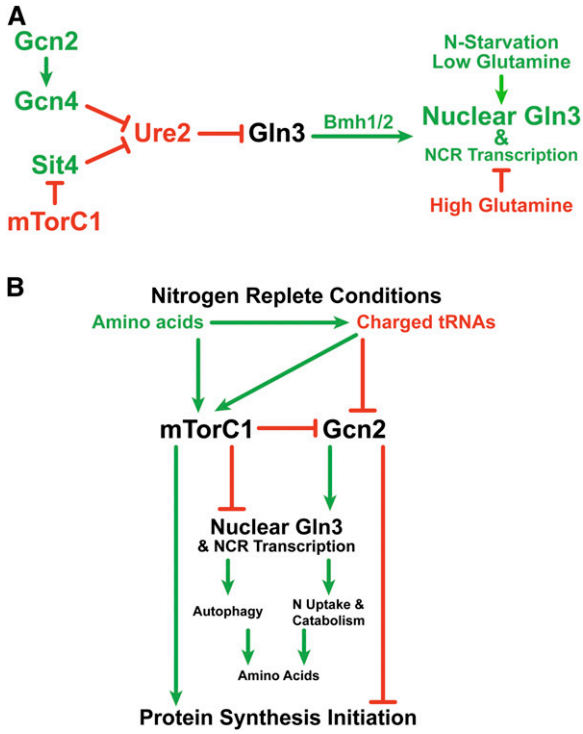

Figure 17 Schematic summary of results obtained from experiments presented in this and earlier work. (A) Epistatic relationships of the genes encoding mTorC1, Sit4, Ure2, Gcn2, Gcn4, and Bmh1/2 in the regulation of NCR-sensitive Gln3 localization. Green arrows and designations indicate positive regulation, whereas red bars and designations indicate negative regulation. (B) Description of the global relationships of mTorC1- and Gcn2-mediated regulation on Gln3 localization and protein synthesis when cells are grown in nitrogen-replete medium.

(Hofman-Bang 1999; Cooper 2002, 2004; Magasanik and Kaiser 2002).

Participation of Bmh1/2 in Gln3 localization and function

The alteration of Gln3 phosphorylation levels by rapamycin and Msx treatments, nitrogen and carbon starvation, nitrogen source identity, as well as abolishment of Sit4 and PP2A subunits, all contributed to our interest in and investigation of the phospho-protein binding 14-3-3 proteins Bmh1/2 (Xiao *et al.* 1995; Muslin *et al.* 1996). Growth was poor in *bmh1*Δ,*bmh2*Δ under all conditions so that characteristic in itself was not informative. On the other hand, nuclear Gln3 localization was significantly diminished and NCR-sensitive transcription abolished in a *bmh1*Δ,*bmh2*Δ mutant. This suggests that Bmh1/2 may well bind to a phosphorylated form of Gln3. Consistent with this suggestion, MS analyses by Kakiuchi *et al.* (2007) show that Bmh2 and Gln3 interact with one another. One may speculate that a Bmh1/2-Gln3 interaction would stabilize the phosphorylated form of Gln3, and hence their loss would increase Gln3 dephosphorylation as we observe. A formally similar argument was made with respect to the Gln3-Ure2 interaction (Bertram *et al.* 2000). This, however, does not explain the function of Bmh1/2. The conclusion that Bmh1/2 likely functions downstream of Ure2 and the possibility that the loss of nuclear Gln3-GFP localization in *bmh1*Δ,*bmh2*Δ cells was not as absolute as NCR-sensitive transcription raises the pivotal question of whether Bmh1/2 function prior to or after Gln3 enters the nucleus.

Open questions: the functions of Gcn2, Gcn4, Bmh1/2, and their effects on Gln3 phosphorylation

The participation of Gcn4 in Gln3 control was a surprise. How could Gcn4, a highly characterized transcription activator, influence intracellular Gln3 localization? It is true that Gcn4 collaborates with Gln3 in upregulating the expression of a limited number of NCR-sensitive genes containing binding sites for both transcription factors in their promoters, as well as those encoding *GLN3* and *GAT1* (Mitchell and Magasanik 1984; Natarajan, *et al.* 2001; Valenzuela *et al.* 2001, data set URL is no longer active; Riego *et al.* 2002; Staschke *et al.* 2010; Hernández *et al.* 2011). Such collaboration of Gln3 and Gcn4 coactivating transcription might conceptually shift the Gln3 localization balance toward greater dwell times in the nucleus. Hence a *gcn2* or *gcn4* deletion might, by this reasoning, be expected to shift that balance somewhat toward the cytoplasm. This interpretation, however, fails to account for the observation that Gcn2 likely functions upstream rather than downstream of Ure2 and the very strong effects of the *gcn2* and *gcn4* deletions on abolishing nuclear Gln3 localization in nitrogen-poor medium. Such extensive cytoplasmic Gln3 sequestration would *a priori* predict that Gln3- and Gat1-dependent, NCR-sensitive transcription in

general would be uniformly affected across the board when GAAC regulation is altered. This was not observed in the studies mentioned above. While some NCR-sensitive genes responded to altered GAAC regulation, other well-characterized NCR-sensitive genes did not. For example, *GLT1* was weakly induced, *GLN1* expression was repressed, and *GDH3* showed little response to 3-aminotriazole (3AT) treatment (Natarajan *et al.* 2001). *CAR1*, *DAL5*, and *GAP1* did not respond in the comparison GCN4^{C}/*gcn4*Δ (Natarajan *et al.* 2001), and some highly NCR-sensitive genes (*ASP1*; *DAL1*; *DAL4*; *DCG1*; *DUR1,2*; *PUT4*; *ATG8*; *GAT4*; and *DAL80*) were either unaffected or repressed by 3AT treatment (Staschke *et al.* 2010). Deletion of *GCN4* increased expression of *DAL5*, *DAL1*, and *GAP1* in YPD-grown, rapamycin-treated cells (Valenzuela *et al.* 2001). In none of these analyses did Gln3-mediated, NCR-sensitive transcription uniformly correlate with GAAC. In short, these earlier studies did not shed much light on GAAC regulation of Gln3 localization in nitrogen-poor medium for two reasons: (i) The promoters of many of the NCR-sensitive genes, including those above, have been dissected and shown to contain a complex array of *cis*-acting regulatory sites which limit the extent to which transcriptional analyses alone are able to visualize all of the multifactorial regulation that occurs; and (ii) the transcription data were obtained in cells cultured in repressive media, conditions where *GCN2* and *GCN4* deletions do not exhibit demonstrable effects on Gln3 localization.

The second major question concerns the decreased levels of phosphorylation observed in the *bmh1*Δ,*bmh2*Δ, *gcn2*Δ, and *gcn4*Δ mutants. *A priori* this suggests the loss of a phosphorylation function or inhibition of a phosphatase that depends on the GAAC and Bmh1/2 proteins. In this context it is important to note that rapamycin treatment in glutamine-grown cells and deletion of the *GCN2*, *GCN4*, or *BMH1/2* in proline-grown cells generate Gln3 species with indistinguishable mobilities in SDS gels yet exhibit opposite outcomes on Gln3 localization. Therefore, what is the relationship of Gln3 phosphorylation and dephosphorylation as well as Gcn2 Gcn4, Bmh1/2, and Sit4 functions in the regulation of Gln3 localization and Gln3-mediated transcription? Clearly, much more remains to be done before we will have a detailed molecular model of nitrogen-responsive Gln3 regulation which congruently fits all of the existing experimental data.

Acknowledgments

The authors thank Zhengchang Liu, Evelyne Dubois, and Isabelle Georis for mutant strains; Bill Taylor and the University of Tennessee Molecular Resource Center for assistance with the quantitative RT-PCR experiments; and Thomas Cunningham who performed all of the DNA sequencing associated with this work. The Bmh1/2 experiments formed a portion of D.B.'s doctoral thesis. Supported by National Institutes of Health grant GM-3564227.

Literature Cited

Bar-Peled, L. D. M., and D. M. Sabatini, 2014 Regulation of mTORC1 by amino acids. Trends Cell Biol. 24: 400–406.

Beck, T., and M. N. Hall, 1999 The TOR signalling pathway controls nuclear localization of nutrient-regulated transcription factors. Nature 402: 689–692.

Bertram, P. G., J. H. Choi, J. Carvalho, W. Ai, C. Zeng *et al.*, 2000 Tripartite regulation of Gln3p by TOR, Ure2p, and phosphatases. J. Biol. Chem. 275: 35727–35733.

Binda, M., M. P. Péli-Gulli, G. Bonfils, N. Panchaud, J. Urban *et al.*, 2009 The Vam6 GEF controls TORC1 by activating the EGO complex. Mol. Cell 35: 563–573.

Binda, M., G. Bonfils, N. Panchaud, M. P. Péli-Gulli, and C. De Virgilio, 2010 An EGOcentric view of TORC1 signaling. Cell Cycle 9: 221–222.

Blinder, D., P. W. Coschigano, and B. Magasanik, 1996 Interaction of the GATA factor Gln3p with the nitrogen regulator Ure2p in Saccharomyces cerevisiae. J. Bacteriol. 178: 4734–4736.

Bonfils, G., M. Jaquenoud, S. Bontron, C. Ostrowicz, C. Ungermann *et al.*, 2012 Leucyl-tRNA synthetase controls TORC1 via the EGO complex. Mol. Cell 46: 105–110.

Broach, J. R., 2012 Nutritional control of growth and development in yeast. Genetics 192: 73–105.

Cardenas, M. E., N. S. Cutler, M. C. Lorenz, C. J. Di Como, and J. Heitman, 1999 The TOR signaling cascade regulates gene expression in response to nutrients. Genes Dev. 13: 3271–3279.

Carlson, M., and D. Botstein, 1982 Two differentially regulated mRNAs with different 5′ ends encode secreted and intracellular forms of yeast invertase. Cell 28: 145–154.

Carvalho, J., and X. F. Zheng, 2003 Domains of Gln3p interacting with karyopherins, Ure2p, and the target of rapamycin protein. J. Biol. Chem. 278: 16878–16886.

Castilho, B. A., R. Shanmugam, R. C. Silva, R. Ramesh, B. M. Himme *et al.*, 2014 Keeping the eIF2 alpha kinase Gcn2 in check. Biochim. Biophys. Acta 1843: 1948–1968.

Chan, T. F., P. G. Bertram, W. Ai, and X. F. Zheng, 2001 Regulation of APG14 expression by the GATA-type transcription factor Gln3p. J. Biol. Chem. 276: 6463–6467.

Cherkasova, V. A., and A. G. Hinnebusch, 2003 Translational control by TOR and TAP42 through dephosphorylation of eIF2alpha kinase GCN2. Genes Dev. 17: 859–872.

Coffman, J. A., R. Rai, T. Cunningham, V. Svetlov, and T. G. Cooper, 1996 Gat1p, a GATA family protein whose production is sensitive to nitrogen catabolite repression, participates in transcriptional activation of nitrogen-catabolic genes in *Saccharomyces cerevisiae*. Mol. Cell. Biol. 16: 847–858.

Coffman, J. A., R. Rai, D. M. Loprete, T. Cunningham, V. Svetlov *et al.*, 1997 Cross regulation of four GATA factors that control nitrogen catabolic gene expression in *Saccharomyces cerevisiae*. J. Bacteriol. 179: 3416–3429.

Conrad, M., J. Schothorst, H. N. Kankipati, G. Van Zeebroeck, M. Rubio-Texeira *et al.*, 2014 Nutrient sensing and signaling in the yeast Saccharomyces cerevisiae. FEMS Microbiol. Rev. 38: 254–299.

Cooper, T. G., 1982 Nitrogen metabolism in Saccharomyces cerevisiae, pp 39–99 in *Molecular Biology of the Yeast Saccharomyces: Metabolism and Gene Expression*, edited by J. N. Strathern, E. W. Jones, and J. R. Broach. Cold Spring Harbor Laboratory, Cold Spring Harbor, NY.

Cooper, T. G., 2002 Transmitting the signal of excess nitrogen in Saccharomyces cerevisiae from the Tor proteins to the GATA factors: connecting the dots. FEMS Microbiol. Rev. 26: 223–238.

Cooper, T. G., 2004 Integrated regulation of the nitrogen-carbon interface, pp. 225–257 in *Nutrient-Induced Responses in Eukaryotic Cells*, *topics in current genetics*, Vol. 7, edited by J. Winderickx, and P. M. Taylor. Springer-Verlag, Berlin.

Cox, K. H., A. Kulkarni, J. J. Tate, and T. G. Cooper, 2004a Gln3 phosphorylation and intracellular localization in nutrient limitation and starvation differ from those generated by rapamycin inhibition of Tor1/2 in *Saccharomyces cerevisiae*. J. Biol. Chem. 279: 10270–10278.

Cox, K. H., J. J. Tate, and T. G. Cooper, 2002 Cytoplasmic compartmentation of Gln3 during nitrogen catabolite repression and the mechanism of its nuclear localization during carbon starvation in *Saccharomyces cerevisiae*. J. Biol. Chem. 277: 37559–37566.

Cox, K. H., J. J. Tate, and T. G. Cooper, 2004b Actin cytoskeleton is required for nuclear accumulation of Gln3 in response to nitrogen limitation but not rapamycin treatment in *Saccharomyces cerevisiae*. J. Biol. Chem. 279: 19294–19301.

Crespo, J. L., and M. N. Hall, 2002 Elucidating TOR signaling and rapamycin action: lessons from *Saccharomyces cerevisiae*. Microbiol. Mol. Biol. Rev. 66: 579–591.

Crespo, J. L., T. Powers, B. Fowler, and M. N. Hall, 2002 The TOR-controlled transcription activators GLN3, RTG1, and RTG3 are regulated in response to intracellular levels of glutamine. Proc. Natl. Acad. Sci. USA 99: 6784–6789.

Cunningham, T. S., R. Andhare, and T. G. Cooper, 2000a Nitrogen catabolite repression of DAL80 expression depends on the relative levels of Gat1p and Ure2p production in *Saccharomyces cerevisiae*. J. Biol. Chem. 275: 14408–14414.

Cunningham, T. S., R. Rai, and T. G. Cooper, 2000b The level of DAL80 expression down-regulates GATA factor-mediated transcription in *Saccharomyces cerevisiae*. J. Bacteriol. 182: 6584–6591.

Dever, T. E., T. G. Kinzy, and G. D. Pavitt, 2016 Mechanism and regulation of protein synthesis in *Saccharomyces cerevisiae*. Genetics 203: 65–107.

Di Como, C. J., and K. T. Arndt, 1996 Nutrients, via the Tor proteins, stimulate the association of Tap42 with type 2A phosphatases. Genes Dev. 10: 1904–1916.

Fayyad-Kazan, M., A. Fellera, E. Bodo, M. Boeckstaens, A. M. Marini *et al.*, 2016 Yeast nitrogen catabolite repression is sustained by signals distinct from glutamine and glutamate reservoirs. Mol. Microbiol. 99: 360–379.

Feller, A., I. Georis, J. J. Tate, T. G. Cooper, and E. Dubois, 2013 Alterations in the Ure2 αCap domain elicit different GATA factor responses to rapamycin treatment and nitrogen limitation. J. Biol. Chem. 288: 1841–1855.

Garcia-Barrio, M., J. Dong, S. Ufano, and A. G. Hinnebusch, 2000 Association of GCN1–GCN20 regulatory complex with the N-terminus of eIF2alpha kinase GCN2 is required for GCN2 activation. EMBO J. 19: 1887–1899.

Georis, I., J. J. Tate, T. G. Cooper, and E. Dubois, 2008 Tor pathway control of the nitrogen-responsive DAL5 gene bifurcates at the level of Gln3 and Gat1 regulation in Saccharomyces cerevisiae. J. Biol. Chem. 283: 8919–8929.

Georis, I., J. J. Tate, T. G. Cooper, and E. Dubois, 2011a Nitrogen-responsive regulation of GATA protein family activators Gln3 and Gat1 occurs by two distinct pathways, one inhibited by rapamycin and the other by methionine sulfoximine. J. Biol. Chem. 286: 44897–44912.

Georis, I., J. J. Tate, A. Feller, T. G. Cooper, and E. Dubois, 2011b Intranuclear function for protein phosphatase 2A: Pph21 and Pph22 are required for rapamycin-induced GATA factor binding to the *DAL5* promoter in yeast. Mol. Cell. Biol. 31: 92–104.

Hardwick, J. S., F. G. Kuruvilla, J. K. Tong, A. F. Shamji, and S. L. Schreiber, 1999 Rapamycin-modulated transcription defines the subset of nutrient-sensitive signaling pathways directly controlled by the Tor proteins. Proc. Natl. Acad. Sci. USA 96: 14866–14870.

Hernández, H., C. Aranda, L. Riego, and A. González, 2011 Gln3-Gcn4 hybrid transcriptional activator determines catabolic and biosynthetic gene expression in the yeast *Saccharomyces cerevisiae*. Biochem. Biophys. Res. Commun. 404: 859–864.

Hinnebusch, A. G., 2005 Translational regulation of GCN4 and the general amino acid control of yeast. Annu. Rev. Microbiol. 59: 407–450.

Hofman-Bang, J., 1999 Nitrogen catabolite repression in *Saccharomyces cerevisiae*. Mol. Biotechnol. 12: 35–73.

Huang, W. P., S. V. Scott, J. Kim, and D. J. Klionsky, 2000 The itinerary of a vesicle component, Aut7p/Cvt5p, terminates in the yeast vacuole via the autophagy/Cvt pathways. J. Biol. Chem. 275: 5845–5851.

Ito, H., Y. Fukuda, K. Murata, and A. Kimura, 1983 Transfomation of intact yeast cells treated with alkali ions. J. Bacteriol. 53: 163–168.

Jiang, Y., and J. R. Broach, 1999 Tor proteins and protein phosphatase 2A reciprocally regulate Tap42 in controlling cell growth in yeast. EMBO J. 18: 2782–2792.

Kakiuchi, K., Y. Yamauchi, M. Taoka, M. Iwago, T. Fujita *et al.*, 2007 Proteomic analysis of in vivo 14-3-3 interactions in the yeast *Saccharomyces cerevisiae*. Biochemistry 46: 7781–7792.

Kemp, A. J., R. Betney, L. Ciandrini, A. C. Schwenger, M. C. Romano *et al.*, 2013 A yeast tRNA mutant that causes pseudohyphal growth exhibits reduced rates of CAG codon translation. Mol. Microbiol. 87: 284–300.

Kim, J., and K.-L. Guan, 2011 Amino acid signaling in TOR activation. Annu. Rev. Biochem. 80: 1001–1032.

Kirisako, T., M. Baba, N. Ishihara, K. Miyazawa, M. Ohsumi *et al.*, 1999 Formation process of autophagosome is traced with Apg8/Aut7p in yeast. J. Cell Biol. 147: 435–446.

Krishnamurthy, N., M. R. Meyer, B. M. Jackson, D. Slade, C. Roberts *et al.*, 2001 Transcriptional profiling shows that Gcn4p is a master regulator of gene expression during amino acid starvation in yeast. Mol. Cell. Biol. 21: 4347–4368.

Kulkarni, A. A., A. T. Abul-Hamd, R. Rai, H. El Berry, and T. G. Cooper, 2001 Gln3p nuclear localization and interaction with Ure2p in *Saccharomyces cerevisiae*. J. Biol. Chem. 276: 32136–32144.

Kulkarni, A. A., T. D. Buford, R. Rai, and T. G. Cooper, 2006 Differing responses of Gat1 and Gln3 phosphorylation and localization to rapamycin and methionine sulfoximine treatment in *Saccharomyces cerevisiae*. FEMS Yeast Res. 6: 218–229.

Lageix, S., J. Zhang, S. Rothenburg, and A. G. Hinnebusch, 2015 Interaction between the tRNA-binding and C-terminal domains of Yeast Gcn2 regulates kinase activity in vivo. PLoS Genet. 11: e1004991.

Lamming, D. W., and D. M. Sabatini, 2013 A Central role for mTOR in lipid homeostasis. Cell Metab. 18: 465–469.

Laplante, M., and D. M. Sabatini, 2012 mTOR signaling in growth control and disease. Cell 149: 274–293.

Liu, Z., T. Sekito, M. Spirek, J. Thornton, and R. A. Butow, 2003 Retrograde signaling is regulated by the dynamic interaction between Rtg2p and Mks1p. Mol. Cell 12: 401–411.

Liu, Z., M. Spirek, J. Thornton, and R. A. Butow, 2005 A novel degron-mediated degradation of the RTG pathway regulator, Mks1p, by SCFGrr1. Mol. Biol. Cell 16: 4893–4904.

Ljungdahl, P. O., and B. Daignan-Fornier, 2012 Regulation of amino acid, nucleotide, and phosphate metabolism in Saccharomyces cerevisiae. Genetics 190: 885–929.

Loewith, R., and M. N. Hall, 2011 Target of Rapamycin (TOR) in nutrient signaling and growth control. Genetics 189: 1177–1201.

Magasanik, B., and C. A. Kaiser, 2002 Nitrogen regulation in Saccharomyces cerevisiae. Gene 290: 1–18.

Miller, S. M., and B. Magasanik, 1991 Role of the complex upstream region of the GDH2 gene in nitrogen regulation of the NAD-linked glutamate dehydrogenase in Saccharomyces cerevisiae. Mol. Cell. Biol. 11: 6229–6247.

Mitchell, A. P., and B. Magasanik, 1984 Three regulatory systems control production of glutamine synthetase in *Saccharomyces cerevisiae*. Mol. Cell. Biol. 4: 2767–2773.

Muslin, A. J., J. W. Tanner, P. M. Allen, and A. S. Shaw, 1996 Interaction of 14-3-3 with signaling proteins is mediated by the recognition of phosphoserine. Cell 84: 889–897.

Natarajan, K., M. R. Meyer, B. M. Jackson, D. Slade, C. Roberts *et al.*, 2001 Transcriptional profiling shows that Gcn4p is a master regulator of gene expression during amino acid starvation in yeast. Mol. Cell. Biol. 21: 4347–4368.

Noda, T., and Y. Ohsumi, 1998 Tor, a phosphatidylinositol kinase homologue, controls autophagy in yeast. J. Biol. Chem. 273: 3963–3966.

Parua, P. K., and E. T. Young, 2014 Binding and transcriptional regulation by 14-3-3 (Bmh) proteins requires residues outside of the canonical motif. Eukaryot. Cell 13: 21–30.

Parua, P. K., S. Ratnakumar, K. A. Braun, K. M. Dombek, E. Arms *et al.*, 2010 14-3-3 (Bmh) proteins inhibit transcription activation by Adr1 through direct binding to its regulatory domain. Mol. Cell. Biol. 30: 5273–5283.

Rai, R., J. J. Tate, D. R. Nelson, and T. G. Cooper, 2013 *gln3* mutations dissociate responses to nitrogen limitation (nitrogen catabolite repression) and rapamycin inhibition of TorC1. J. Biol. Chem. 288: 2789–2804.

Rai, R., J. J. Tate, K. Shanmuganatham, M. M. Howe, and T. G. Cooper, 2014 A domain in the transcription activator Gln3 specifically required for rapamycin responsiveness. J. Biol. Chem. 289: 18999–19018.

Rai, R., J. J. Tate, K. Shanmuganatham, M. M. Howe, D. Nelson *et al.*, 2015 Nuclear Gln3 import is regulated by nitrogen catabolite repression whereas export is specifically regulated by glutamine. Genetics 201: 989–1016.

Rai, R., J. J. Tate, and T. G. Cooper, 2016 Multiple targets on the Gln3 transcription activator are cumulatively required for control of its cytoplasmic sequestration. G3 6: 1391–1408.

Riego, L., A. Avendaño, A. DeLuna, E. Rodríguez, and A. González, 2002 GDH1 expression is regulated by GLN3, GCN4, and HAP4 under respiratory growth. Biochem. Biophys. Res. Commun. 293: 79–85.

Roberts, R. L., H. U. Mösch, and G. R. Fink, 1997 14-3-3 proteins are essential for RAS/MAPK cascade signaling during pseudohyphal development in S. cerevisiae. Cell. 89: 1055–1065.

Robertson, L. S., H. C. Causton, R. A. Young, and G. R. Fink, 2000 The yeast A kinases differentially regulate iron uptake and respiratory function. Proc. Natl. Acad. Sci. USA 97: 5984–5988.

Schmelzle, T., T. Beck, D. E. Martin, and M. N. Hall, 2004 Activation of the RAS/cyclic AMP pathway suppresses a TOR deficiency in yeast. Mol. Cell. Biol. 24: 338–351.

Schmitt, M. E., T. A. Brown, and B. L. Trumpower, 1990 A rapid and simple method for preparation of RNA from *Saccharomyces cerevisiae*. Nucleic Acids Res. 18: 3091–3092.

Shimobayashi, M., and M. N. Hall, 2016 Multiple amino acid sensing inputs to mTorC1. Cell Res. 26: 7–20.

Sosa, E., C. Aranda, L. Riego, L. Valenzuela, A. DeLuna *et al.*, 2003 Gcn4 negatively regulates expression of genes subjected to nitrogen catabolite repression. Biochem. Biophys. Res. Commun. 310: 1175–1180.

Staschke, K. A., S. Dey, J. M. Zaborske, L. R. Palam, J. N. McClintick *et al.*, 2010 Integration of general amino acid control and target of rapamycin (TOR) regulatory pathways in nitrogen assimilation in yeast. J. Biol. Chem. 285: 16893–16911.

Stauffer, B., and T. Powers, 2016 Target of rapamycin signaling mediates vacuolar fragmentation. Curr. Genet. DOI: 10.1007/s00294-016-0616-0.

Swinnen, E., R. Ghillebert, T. Wilms, and J. Winderickx, 2014 Molecular mechanisms linking the evolutionary conserved TORC1-Sch9 nutrient signalling branch to lifespan regulation in *Saccharomyces cerevisiae*. FEMS Yeast Res. 14: 17–32.

Tate, J. J., and T. G. Cooper, 2003 Tor1/2 regulation of retrograde gene expression in Saccharomyces cerevisiae derives indirectly as a consequence of alterations in ammonia metabolism. J. Biol. Chem. 278: 36924–36933.

Tate, J. J., and T. G. Cooper, 2007 Stress-responsive Gln3 localization in *Saccharomyces cerevisiae* is separable from and can overwhelm nitrogen source regulation. J. Biol. Chem. 282: 18467–18480.

Tate, J. J., and T. G. Cooper, 2013 Five conditions commonly used to down-regulate tor complex 1 generate different physiological situations exhibiting distinct requirements and outcomes. J. Biol. Chem. 288: 27243–27262.

Tate, J. J., A. Feller, E. Dubois, and T. G. Cooper, 2006 *Saccharomyces cerevisiae* Sit4 phosphatase is active irrespective of the nitrogen source provided, and Gln3 phosphorylation levels become nitrogen source-responsive in a *sit4*-deleted strain. J. Biol. Chem. 281: 37980–37992.

Tate, J. J., I. Georis, A. Feller, E. Dubois, and T. G. Cooper, 2009 Rapamycin-induced Gln3 dephosphorylation is insufficient for nuclear localization: Sit4 and PP2A phosphatases are regulated and function differently. J. Biol. Chem. 284: 2522–2534.

Tate, J. J., I. Georis, E. Dubois, and T. G. Cooper, 2010 Distinct phosphatase requirements and GATA factor responses to nitrogen catabolite repression and rapamycin treatment in *Saccharomyces cerevisiae*. J. Biol. Chem. 285: 17880–17895.

Tate, J. J., I. Georis, R. Rai, F. Vierendeels, E. Dubois *et al.*, 2015a GATA factor regulation in excess nitrogen occurs independently of Gtr-Ego complex-dependent TorC1 activation. G3 (Bethesda) 5: 1625–1638.

Tate, J. J., R. Rai, and T. G. Cooper, 2015b Nitrogen starvation and TorC1 inhibition differentially affect nuclear localization of the Gln3 and Gat1 transcription factors through the rare glutamine $tRNA_{CUG}$ in *Saccharomyces cerevisiae*. Genetics 199: 455–474.

Valenzuela, L., C. Aranda, and A. Gonzalez, 2001 TOR modulates GCN4-dependent expression of genes turned on by nitrogen limitation. J. Bacteriol. 183: 2331–2334.

van Heusden, G. P., 2009 14-3-3 Proteins: insights from genome-wide studies in yeast. Genomics 94: 287–293.

van Heusden, G. P., and H. Y. Steensma, 2006 Yeast 14-3-3 proteins. Yeast 23: 159–171.

Wach, A., A. Brachat, R. Pöhlmann, and P. Philippsen, 1994 New heterologous modules for classical or PCR-based gene disruptions in Saccharomyces cerevisiae. Yeast 10: 1793–1808.

Wang, H., X. Wang, and Y. Jiang, 2003 Interaction with Tap42 is required for the essential function of Sit4 and type 2A phosphatases. Mol. Biol. Cell 14: 4342–4351.

Watson, T. G., 1977 Inhibition of proline utilization by glutamate during steady state growth of *Saccharomyces cerevisiae*. J. Gen. Microbiol. 103: 123–126.

Xiao, B., S. J. Smerdon, D. H. Jones, G. G. Dodson, Y. Soneji *et al.*, 1995 Structure of a 14-3-3 protein and implications for coordination of multiple signalling pathways. Nature 376: 188–191.

Yan, G., X. Shen, and Y. Jiang, 2006 Rapamycin activates Tap42-associated phosphatases by abrogating their association with Tor complex 1. EMBO J. 25: 3546–3555.

Communicating editor: M. Hampsey